Cumulative impact assessment of collisions with existing and planned offshore wind turbines in the southern North Sea

Analysis of additional mortality using collision rate modelling and impact assessment based on population modelling for the KEC 4.0

Deze werkversie is bedoeld als input voor het Programma Noordzee 2022-2027, en is opgesteld met de best beschikbare kennis d.d. 1 september 2021. Deze werkversie vervalt bij het openbaar worden van de KEC 4.0 documenten.

Commissioned by: Rijkswaterstaat Water, Verkeer en Leefomgeving

15 Oct. 2021
report nr 21-205

Cumulative impact assessment of collisions with existing and planned offshore wind turbines in the southern North Sea

Analysis of additional mortality using collision rate modelling and impact assessment based on population modelling for the KEC 4.0

dr. A. Potiek, J.J. Leemans *MSc*., R.P. Middelveld *MSc*., dr. A. Gyimesi

Status: draft

Report nr:	21-205
Project nr:	20-1096
Date of publication:	15 Oct. 2021
Photo credits cover page:	Name / names / Bureau Waardenburg bv
Project manager:	dr. Abel Gyimesi
Second reader:	Ruben Fijn, *MSc.*
Name & address client:	Rijkswaterstaat Water, Verkeer en Leefomgeving Griffioenlaan 2 3526 LA UTRECHT
Reference client:	zaak 31167080
Signed for publication:	Team Manager Bureau Waardenburg bv R.C. Fijn, *MSc.*
Signature:	

Please cite as: Potiek, A., J.J., Leemans, R.P. Middelveld & A. Gyimesi, 2021. Cumulative impact assessment of collisions with existing and planned offshore wind turbines in the southern North Sea. Analysis of additional mortality using collision rate modelling and impact assessment based on population modelling for the KEC 4.0. Rapportnr. 21-205. Bureau Waardenburg, Culemborg.

Keywords: offshore wind, windturbine, collision, seabird, acceptable level of impact, Southern North Sea

Bureau Waardenburg
Ecology & Landscape

Bureau Waardenburg, Varkensmarkt 9, 4101 CK Culemborg, the Netherlands
0031 (0) 345 512 710, info@buwa.nl, www.buwa.nl

Table of contents

1 Introduction

1.1 Background

The intended developments of offshore wind energy in the Dutch North Sea up to 2030 including an additional 10 GW may lead to cumulative effects on seabird species, in terms of estimated numbers of collision victims. In the Framework for Assessing Ecological and Cumulative Effects (in short KEC; cf. the Dutch abbreviation), the cumulative effects of all existing and planned Dutch and foreign wind farms are predicted and evaluated. This was done in 2015 in KEC 1.0 for offshore wind developments until 2023 covering a large number of bird species with a protected status (Rijkswaterstaat 2015). In 2019, this exercise was updated for the Roadmap for Offshore Wind Energy 2030 (Rijkswaterstaat 2019), to also include plans for offshore wind farms up to 2030 in the calculations.

In the 'North Sea Programme 2022-2027', search areas for new offshore wind energy areas are designated (approx. 27 GW), which will be used for the Roadmap 2040. For now 10 GW is needed before 2030 to achieve the aims set in the Energy Agenda. In order to be able to realize this further development of offshore wind energy in accordance with the Energy Agenda, the KEC needed to be actualised with the most recent knowledge. This concerns, among other things, the application of new insights into the occurrence and flight behaviour of birds in the North Sea, carrying out calculations with the most recent models and evaluate the effects against the Acceptable Level of Impact (ALI). Moreover, new wind energy search areas were defined for options for accelerated development up to 2030. The effects of these search areas in terms of numbers of bird victims need to be calculated in combination with existing and planned wind farms up to 2030 according to the most realistic possible assumptions.

1.2 Objective

The aim of the report at hand is to calculate the population level effects of bird collisions in wind farms taken up in the 'North Sea Programme' 2022-2027 for a number of relevant bird species. The calculations have been actualised based on the most recent knowledge. Subsequently, the calculated numbers of casualties have been projected against acceptable standards, providing insight into whether the development of offshore wind remains within the ecological constraints.

2 Materials and methods

2.1 Wind farm scenarios

We performed impact assessments for different wind farm scenarios, provided by Rijkswaterstaat (Table 2.1). These consist of a null model representing the unimpacted scenario, four scenarios with combinations of wind farms on the Dutch Continental Shelf encompassing existing and ‘realistic’ wind farms until 2030 (part of Roadmap 2030; Table 2.2), the new search areas of the North Sea Programme (Table 2.2), and one scenario including international wind farms. All currently simulated scenarios are based on the roadmap up to 2030. In a later stage, the impact assessment for roadmap 2040 will be carried out.

Table 2.1 Wind farm scenarios used in this study, as provided by Rijkswaterstaat.

Scenario name	Bird densities	Description
null	-	scenario without wind farms
Basic nat 30	national	basic: existing and realistic wind farms up to 2030
Rekenvariant I	national	basic + 10.7 GW, restricted option (commissioned by Ministry of Infrastructure and Water Management)
Rekenvariant II	national	basic + 12.7 GW, fallback option
Rekenvariant III	national	basic + 16.7 GW, favoured
Int 30	international	basic nat 30 + Rekenvariant III + all international wind farms planned with starting date until end 2030

Table 2.2 Wind farms being part of the Roadmap 2030, forming the basic scenario and taken up in each future scenario.

Wind farm
Borssele I-V
Egmond aan Zee
Prinses Amaliawindpark
Eneco Luchterduinen
Gemini
Hollandse Kust Zuid I-IV
Hollandse Kust Noord
Ten noorden v. d. Waddeneilanden
Hollandse Kust West
IJmuiden Ver

Table 2.3 Wind farm search areas taken up in the North Sea Programme. Combinations of these search areas form the different future scenarios.

Wind farm	Basic nat 30	Rekenvariant I	Rekenvariant II	Rekenvariant III
Hollandse Kust West zuidelijke punt	-	X	X	X
Zoekgebied 1 Noord	-	-	-	X
IJmuiden Ver Noord	-	X	X	X
Zoekgebied 1 Zuid	-	-	X	X
Zoekgebied 2 Noord	-	X	X	X
Zoekgebied 5 Oost	-	X	X	X

2.2 Estimating number of victims using collision rate modelling

Numbers of victims were first estimated for each wind farm, and then summed over the wind farms according to the different scenarios. The approach of estimating the numbers of victims differed between seabirds and migratory birds.

2.2.1 Seabirds

Collision mortality was calculated for ten seabird species:

- Great black-backed gull
- Lesser black-backed gull
- Herring gull
- Little gull
- Black-legged kittiwake
- Northern gannet
- Great skua
- Arctic skua
- Common tern
- Sandwich tern

International versus national densities

Densities of seabirds are calculated for two scales: international and national densities. Input for the international densities were ESAS (European Seabirds At Sea) ship-based and aerial survey data from 1991 to 2020. This relatively long period was chosen due to strong variation between counts, as well as due to limited data availability. For the calculations of national densities, MWTL (Monitoring Waterstaatkundige Toestand des Lands) aerial survey data have been used. As these aerial MWTL data are collected at relatively small intervals (2 months) and cover the entire Dutch part of the North Sea in great detail, the density estimates from these surveys are considered more reliable for the

Netherlands than those from the ESAS data. In order to have surveys conducted according to the same methodology and avoid using surveys from the far past in the calculations of mean densities, we decided to select a shorter period of data collection (1999-2020) for the analyses.

In order to generate the density maps, different datasets were used for different species (cf. Rijkswaterstaat 2015). Namely, high concentrations of northern gannets, black-legged kittiwakes, herring gulls, great black-backed gulls and lesser black-backed gulls behind fishing vessels were spread out in space in the first iteration of the KEC 1.0 (Leopold *et al.* 2015).. The reliability of the analyses was improved further in a second iteration (van der Wal *et al.* 2015) by basing the density calculations for large gulls in the Netherlands exclusively on MWTL aircraft counts.

Flux determination

Based on the two scales described above, Wageningen Marine Research (WMR) determined bimonthly species densities in a grid of 5 x 5 km by interpolating the count data. A long-term average over the whole study period (*i.e.,* 1991-2020 for the international scenario and 1999-2020 for the national scenarios) was calculated for each bimonthly period and for each grid cell to create density maps per species. Subsequently, the wind farm layouts were projected over these bird density maps. The average species-specific bimonthly density per wind farm was calculated over all grid cells overlapping with the wind farm layout.

The basic input parameter for the collision risk calculations is the wind farm- and species-specific flux flying through the particular rotor swept area of that wind farm. This flux of flying birds was for seabirds based on the local density of each species in each wind farm. However, the ESAS methodology that was used to collect the density data leads to a tendency to underestimate the number of flying birds. Therefore, the total density (*i.e.,* swimming and flying birds together) in each wind farm in each bimonthly period was multiplied by a species-specific correction factor, accounting for the mean fraction of the time budget that particular bird species tends to spend in the air. For most species, this mean fraction of time flying (Table 2.4) was based on a study of Maclean *et al.* (2009). The correction factor as determined by Collins *et al.* (2016) was used for black-legged kittiwake and the factors as determined by Gyimesi *et al.* (2017b) were used for the lesser black-backed gull and herring gull. A study with GPS-loggers in the United Kingdom provided the fraction of time flying for the northern gannet (Cleasby *et al.* 2015), while another GPS-study in Canada is the source of the value for the great black-backed gull (Maynard 2018).

These densities were transformed into fluxes at rotor height, based on species-specific flight height distributions relative to the turbine specifications (*i.e.,* hub height and rotor diameter). Bird-related data like flight height distributions are specified in §2.3.1, while turbine specifications are discussed in §2.3.2.

2.2.2 Migratory birds

In addition to seabird species, collision victims in offshore wind farms were also calculated for several migratory bird species. In contrast to seabird species, offshore areas are not the natural habitat of these species. However, during seasonal migration, they cross the central and southern North Sea and hence may collide with wind turbines in offshore wind farms. The following eight species have been identified as priority species for which collision victims were calculated in the present study:

- Bewick's swan
- Brent goose
- Common shelduck
- Curlew
- Red knot
- Bar-tailed godwit
- Black tern
- Common starling

There is no systematic monitoring of migratory birds at sea and therefore no location-specific offshore densities or fluxes are available. Therefore, a generic flux across the southern North Sea was estimated for migratory birds in KEC 1.1, providing the basis for the calculations of numbers of victims for each wind farm (Rijkswaterstaat 2015). In accordance with the KEC 3.0 study, these fluxes were corrected for the present study based on the percentual change in population size estimates (BirdLife International 2004, 2015). Furthermore, for Bewick's swan and brent goose species-specific migration routes were determined based on GPS logger data (Gyimesi *et al.* 2017a). For black tern the offshore occurrence of birds on migration was based on an analysis of the ESAS database (Potiek *et al.* 2019b). Based on these migration routes, also the total length of the migration corridor could be adjusted, allowing the correction of the KEC 1.1 fluxes into wind farm-specific fluxes. No such detailed measurements were available for the other species and hence generic fluxes for all wind farms were used for these species (Table 2.3).

Table 2.3 Fluxes used in the collision risk calculations in the KEC 1.1 and KEC 3.0 studies (Rijkswaterstaat 2015, 2019) and in the present study. Note that three species were not actualised in KEC 3.0 (-).

species	flux in KEC 1.1 (2015)	flux in KEC 3.0 (2019)	flux in present study
Bewick's swan	43	43	37
brent goose	432	432	589
common shelduck	576	644	644
curlew	742	645	645
red knot	1,349	-	1,434
bar-tailed godwit	742	-	742
black tern	674	608	681
common starling	38,400	-	39,469

2.3 Collision calculations

The numbers of collision victims were calculated using the stochastic Collision Risk Model (hereafter the ‘sCRM’). This model is based on the SOSS Band model (Band 2012) but allows more detailed input data to be used, specifically in relation to modelling variability around certain parameters (Marine Scotland 2018). This translates into a range of estimates being produced, as opposed to single figures. Therefore, the model has the ability to calculate standard deviations around the mean monthly numbers of expected collisions. This gives an indication of the uncertainty around the estimated collision rate. For each species, 1,000 iterations have been run.

The sCRM requires several input parameters related to the characteristics of the bird species and the wind turbines to calculate the theoretical collision risk of each species per type of wind turbine. The calculated species-specific collision risk is then multiplied by the species-specific bird flux through the total rotor-swept area of each wind farm and adjusted for the species-specific avoidance behaviour. The estimated number of collision victims per wind farm and per bird species is subsequently calculated for each month.

For most species, a species-specific flight height distribution was available which allowed the application of the sCRM. No species-specific height distributions were available for the common shelduck, curlew, red knot, bar-tailed godwit, black tern and common starling. Therefore, for these latter species the basic Band model was used (Band *et al.* 2007) in line with the previous KEC studies (Rijkswaterstaat 2015, 2019). All sCRM simulations were performed in R (R Core Team 2019). The original code of the model was slightly adapted to allow calculations for migratory birds in addition to seabirds.

2.3.1 Bird data

As a part of the present study, a literature review was carried out for each species separately, to update the knowledge base of bird parameters used in the sCRM and the population models. The outcome of this literature review will be reported in more detail in the future. Within this report, we only provide the figures selected to be used in the model. Table 2.4 provides a summary of all these bird-related figures used in the calculations. We incorporated variability in the body length, wingspan and flight speed of each species by adding standard deviations. Based on these range of values (following a normal (zero-truncated) distribution with given mean and standard deviation), the model randomly sampled a value for these parameters for each iteration. Means and standard deviations of **body length** and **wingspan** of each species were calculated based on ranges given by Snow and Perrins (eds) (1998) and the assumptions that the middle of this range was the mean value and that all data falls within three standard deviations from the mean.

The means and standard deviations of **flight speeds** of herring gull and lesser black-backed gull were calculated based on data from GPS tags placed on birds in Dutch, Belgian, and British colonies around the Southern North Sea (Gyimesi *et al.* 2017b), while we used flight speeds for great black-backed gull, little gull and arctic skua as reported in Alerstam *et al.* (2007) and for great skua and northern gannet as reported in Pennycuick

(1990). For black-legged kittiwake we used two different values of flight speed for flux and collision risk calculations respectively, as recommended by Skov *et al.* (2018). Flight speeds of Bewick's swan and brent goose were recalculated for this study based on data from Gyimesi *et al.* (2017b). Similarly, flight speeds of curlew and red knot were calculated from raw GPS-data from studies of Schwemmer *et al.* (2016) and Duijns *et al.* (2017). A recent study of Green *et al.* (2021) reported on the flight speed of shelducks crossing the North Sea. For bar-tailed godwit and starling we used flight speeds of Pennycuick *et al.* (2013). Flight speeds of common tern, black tern and sandwich tern also originate from literature (Wakeling & Hodgson 1992; Blake & Chan 2006; Fijn & Gyimesi 2018 respectively).

Due to a lack of data, we did not incorporate standard deviations for nocturnal activity and avoidance. **Nocturnal activity** of lesser black-backed gull and herring gull was based on Gyimesi *et al.* (2017a) and of northern gannet on Furness *et al.* (2018). In the case of Sandwich tern, nocturnal activity was based on unpublished data of Collier, while the assumptions of Garthe and Hüppop (2004) were adopted for the other species. **Avoidance rates** for most seabird species were based on a review of Cook *et al.* (2018). For the other seabird species and all migratory species, we used avoidance rates based on Maclean *et al.* (2009), which is in line with the previous KEC studies (Rijkswaterstaat 2015, 2019).

The sCRM has the ability to randomly sample a **flight height distribution** in each iteration from a catalogue of different flight height distributions. Therefore, we incorporated more variability in the model by adding different flight height distributions for each species. Flight height distributions of lesser black-backed gull and herring gull were calculated based on data from GPS tags placed on birds in Dutch, Belgian, and British colonies around the Southern North Sea (Gyimesi *et al.* 2017a). We used a separate distribution for each individual bird with more than 1,500 data points. The same method was applied to generate different flight height distributions for great skua and northern gannet based on GPS-data of Ross-Smith *et al.* (2016) and Cleasby *et al.* (2015), respectively. For great black-backed gull, we sampled from two different distributions from Swedish and Danish logger data (Gyimesi *et al.* 2017b), and one distribution as used in the previous KEC studies, which is based on Johnston *et al.* (2014). For all other seabird species, we generated 200 different flight height distributions by sampling from a zero-truncated normal distribution, with means and standard deviations based on 95% confidence intervals presented per height class in Johnston *et al.* (2014). Lastly, flight height distributions of Bewick's swan and brent goose were based on data from Gyimesi *et al.* (2017b).

Table 2.4 *Parameters used in the sCRM calculations in this study. Nocturnal activity and fraction of time in flight was only used for seabird species. The basic Band model was used for the species with a given fraction of birds at rotor height. For Bewick's swan and brent goose, concrete fluxes at rotor height were used in the Band model, which therefore did not need to be corrected for nocturnal activity and fraction of time in flight. Note that for black-legged kittiwake two different values of flight speed were used for flux calculation and collision risk calculation. Data sources for the various parameters are stated as letters in the table and shown below it.*

	body length (m)[a]		wingspan (m)[a]		flight speed (m/s)		nocturnal activity	avoidance (%)	fraction at rotor height[r]	fraction time in flight
species	**mean**	**sd**	**mean**	**sd**	**mean**	**sd**				
herring gull	0.60	0.015	1.44	0.020	11.34[b]	3.91[b]	0.01[b]	99.5[c]		0.3[b]
great black-backed gull	0.71	0.023	1.58	0.025	13.7[d]	1.20[d]	0.50[e]	99.5[c]		0.34[f]
lesser black-backed gull	0.58	0.020	1.43	0.025	9.41[b]	3.92[b]	0.43[b]	99.8[c]		0.43[b]
little gull	0.26	0.003	0.78	0.008	11.5[d]	0.10[d]	0.25[e]	99.5[g]		0.6[g]
northern gannet	0.94	0.022	1.73	0.025	14.9[h]	2.60[h]	0.08[i]	98.9[c]		0.82[j]
black-legged kittiwake	0.39	0.003	1.08	0.042	8.71 / 6.22[k]	3.16 / 3.40[k]	0.50[e]	99.2[c]		0.672[l]
arctic skua	0.44	0.008	1.18	0.025	13.8[d]	2.20[d]	0[e]	99.5[g]		1[g]
common tern	0.33	0.007	0.88	0.035	9.2[m]	3.10[m]	0[e]	99.0[g]		1[g]
great skua	0.56	0.008	1.36	0.013	14.9[h]	3.80[h]	0[e]	99.5[g]		0.8[g]
sandwich tern	0.39	0.008	1.00	0.017	10.3[n]	3.40[n]	0.05[o]	99.0[g]		1[g]
bewick's swan	1.21	0.020	1.96	0.052	16.88[p]	0.62[p]		98.0[g]		
brent goose	0.59	0.008	1.15	0.017	17.25[p]	0.27[p]		98.0[g]		
shelduck	0.63	0.015	1.22	0.038	18.21[q]	4.32[q]		98.0[g]	0.5	
curlew	0.55	0.017	0.90	0.033	17.78[s]	3.30[s]		98.0[g]	0.75	
red knot	0.24	0.003	0.59	0.007	16.64[t]	0.56[t]		98.0[g]	0.75	
bar-tailed godwit	0.38	0.003	0.75	0.017	14.4[u]	1.97[u]		98.0[g]	0.75	
black tern	0.23	0.003	0.66	0.007	7.1[v]	0.64[v]		98.0[g]	0.07	
common starling	0.22	0	0.40	0.008	15.4[u]	1.71[u]		98.0[g]	0.5	

[a] Snow & Perrins (1998); [b] Gyimesi *et al.* 2017a; [c] Cook *et al.* 2018; [d] Alerstam *et al.* 2007; [e] Garthe & Hüppop 2004; [f] Maynard 2018; [g] Maclean *et al.* 2009; [h] Pennycuick 1990; [i] Furness *et al.* 2018; [j] Cleasby *et al.* 2015; [k] Skov *et al.* 2018; [l] Collins *et al.* 2016; [m] based on Wakeling & Hodgson 1992; [n] Fijn & Gyimesi 2018; [o] Collier, unpublished; [p] based on Gyimesi *et al.* 2017b; [q] Green *et al.* 2021; [r] Rijkswaterstaat 2015; [s] based on Schwemmer *et al.* 2016; [t] based on Duijns *et al.* 2017; [u] Pennycuick *et al.* 2013; [v] Blake & Chan 2006

2.3.2 Wind farm and wind turbine data

Most of the data on wind farm configurations and the wind turbine specifications were provided by RWS in an Excel file (‘scenario KEC 4.0 versie 8.xlsx’), with an accompanying note (‘Memo Scenario en varianten KEC 4 17-5 definitief.docx’). Missing values of rotation speed, pitch and blade width were calculated based on extrapolation of known figures.

2.4 Impact assessment at population level

2.4.1 Population models

Impacts at population-level were assessed using matrix population models. For this project, population models from Potiek *et al.* (2019) and van Kooten *et al.* (2019) have been adapted, resulting in the R package KEC4popmodels. Within this package, the population growth rate (lambda) for the null scenario without additional mortality due to wind farms is calculated based on demographic rates. Subsequently, the wind farm mortality for the different scenarios (Rekenvariant I to III) was simulated (see §2.1) by adjusting survival rates of the relevant life stages.

2.4.2 Assumptions

Parameter uncertainty
Similar to the previous models used in Potiek *et al.* (2019) and van Kooten *et al.* (2019), input parameters varied between simulations, not between years within a simulation. This is a worst-case approach, which assumes that variation between estimates is due to parameter uncertainty. This assumption resulted in a wider variation in model outputs.

2.4.3 Calculation of mortality fraction

Seabirds
For seabirds, the numbers of collision victims were estimated for each month based on the bimonthly estimates of bird densities. In order to get to an annual estimated mortality fraction, we calculated the average percentage of victims per period (*i.e.,* number of victims in period i / number of individuals present in period i based on density maps * 100%), and extrapolated this average per bimonthly period to a year. Subsequently, this number of victims was divided by the ‘population size’. As the number of victims making use of the area differs per bimonthly period, and part of the individuals present in one period will generally be present in the following as well, we defined the population as follows:

Population seabirds = maximum of average interpolated bimonthly counts

In other words, for each species, the highest bimonthly estimated number of individuals defined the population size. This maximum number of individuals present at any bimonthly period provides a minimum population estimate, as the actual population size can only be larger than the number of birds counted and not smaller. Therefore, this assumption provides a worst-case scenario for the calculation of the mortality fraction (*i.e.,* the smallest possible population size), and thus complies to the requirement of a precautionary approach.

For seabirds, the mortality fraction is calculated for each bimonthly period by dividing the estimated number of victims within a period by the number of individuals present during the same period. As the numbers of individuals present varied between periods, we decided to calculate the average mortality fraction based on the six bimonthly periods, and extrapolate this fraction to a year by the following equation:

$$\text{Mortality fraction seabirds} = \frac{1-(1-\text{average bimonthly mortality})^6}{Population}$$

Migratory birds

Instead of bimonthly counts, the numbers of collision victims for migratory birds were based on estimated fluxes in the autumn, which were based on the size of the flyway population (cf. Rijkswaterstaat 2015). Here, the population was defined as follows:

Population migratory birds = estimated flux in autumn

The flux in autumn is for all species higher than the flux in spring. As part of the individuals in autumn are included in the spring migration as well, the flux in autumn is an indication for the minimum number of individuals making use of the southern North Sea.

For migratory birds, the mortality fraction is calculated as the sum of the number of collision victims in autumn and spring, divided by the population size.

$$\text{Mortality fraction migratory birds} = \frac{\text{Summed number of victims autumn+spring}}{Population}$$

Apportionment of victims

The number of victims per (planned) wind farm is estimated using collision rate models (see §0). This estimate from the BAND model only specifies the total estimated number of victims, without apportioning between age classes.

For the apportionment of victims among age classes, we assumed that the age distribution at sea gives an indication for the age distribution among victims. Estimates of offshore age distribution were available for black-legged kittiwake, little gull, northern gannet, great skua, arctic skua, common tern and black tern (Potiek *et al.* 2019a).

2.4.4 Assessment of impact

The assessment of the impacts was carried out by comparing the outcome of the population models with the species-specific Acceptable Levels of Impact, as defined by the Ministry of

Agriculture, Nature and Food Quality (Table 2.5). The specifications per species were based on (Potiek *et al.* 2021).

Table 2.5 Decisions for Acceptable levels of impact, as defined by the Ministry of Agriculture, Nature and Food Quality (LNV). IUCN status refers to the IUCN World status, based on BirdLife International (2021), with LC = Least Concern, NT = Near Threatened, VU = Vulnerable, EN = Endangered.

Species	IUCN_status	Threshold X after three generations or 10 years	P_T : accepted level of causality
Lesser black-backed gull	LC	30% decline	0.5
Herring gull	VU	15% decline	0.1
Great black-backed gull	LC	30% decline	0.5
Black-legged kittiwake	EN	15% decline	0.1
Little gull	LC	FOR NOW: 30% decline	FOR NOW: 0.5
Northern gannet	LC	30% decline	0.5
Arctic skua	EN	15% decline	0.1
Great skua	LC	30% decline	0.5
Common tern	LC	30% decline	0.5
Sandwich tern	LC	30% decline	0.5
Bewick's swan	EN	15% decline	0.1
Brent goose	LC	30% decline	0.5
Common shelduck	LC	30% decline	0.5
Eurasian curlew	VU	15% decline	0.1
Black tern	LC	30% decline	0.5
Common starling	LC	30% decline	0.5
Bar-tailed godwit	NT	FOR NOW: 15% decline	FOR NOW: 0.1
Red knot	LC	30% decline	0.5

3 Input parameters population models

3.1 General model description and demographic rates per species

Input for the population models consists of estimated stage-specific survival rates, fecundity and fraction non-breeding adults (floaters). Within this project, the knowledge base on demographic rates used within Potiek *et al.* (2019a) was updated to include recent relevant studies.

Within this chapter, the used demographic rates are reported, including data sources. The updated knowledge base is reported in Appendix XXX. Each data source within the updated knowledge base is scored for representativeness and data quality, using the same approach as in Horswill and Robinson (2015) and Potiek *et al.* (2019a).

This approach of Horswill and Robinson (2015) is based on the following criteria to assess data quality:

- Q1) the number of years (>10),
- Q2) the number of individuals and
- Q3) whether an indication of variation between years or areas (standard deviation), or a range of error (standard error) has been reported.

Each of these criteria is scored with 0, 1, or 2: 0 for ‘poor’, 1 for ‘intermediate/unknown’ and 2 for ‘good’.

In a similar way, we assess the representativeness of each data source. This representativeness is scored based on:

- R1) how recent the data are (score 2 for data of less than 10 years old; threshold between score 1 and 0 depends on the species and data availability),
- R2) how representative the area/site is for the Dutch part of the North Sea, and
- R3) how representative the data are for the current local trend in the Dutch part of the North Sea. In our study we used data on population trends since 1990 from Boele et al. (2021) to assess the current local trend of each species.

For each species, the defined stages are described using the following general structure:

- a first-year stage (stage J0),
- followed by one or more immature stages (stages starting with I, for example I1 to I4),
- and an adult stage (stage A).

Demographic rates are reported using the same stage indices, with for example SI1 being the survival of the I1 stage. Fecundity is presented as the number of fledglings per breeding pair. For most species, a fraction floaters is assumed, if possible based on literature. This is depicted in the tables with demographic rates as prob. floater.

Lesser black-backed gull

The population model for lesser black-backed gull consists of a first-year stage (stage J0), four immature stages (I1 to I4), and an adult stage (A). Demographic rates and references are reported in Table 3.1.

Table 3.1 *Demographic rates of null model for lesser black-backed gull. Si indicates the survival rate of stage* i. *Fecundity is presented as the number of fledglings per breeding pair. Prob. floater indicates the probability of non-breeding for an adult. * several projects are currently being carried out to determine additional estimates of especially survival rates (colour-ring programmes in Europe) but also fecundity rates, so this overview is not a complete inventory and additional analyses might yield better estimates.*

	Mean	sd	Reference
SJ0	0.521	0.0375	[1]; [2]; [3]; [4]
SI1	0.856	0.052	[1]; [4]
SI2	0.856	0.052	[1]; [4]
SI3	0.856	0.052	[1]; [4]
SI4	0.856	0.052	[1]; [4]
SA	0.914	0.02	[3]; [4]; [5]; [6]
Fecundity	0.807	0.18	[5]; [7]; [8]; [9]; [10]; [11]; [12]
Prob. floater	0.435	0.1	[1]; [13]

Reference: [1] Camphuysen (2013); [2] Harris (1970); [3] Camphuysen & Gronert (2012); [4] Camphuysen (2011); [5] Wanless et al. (1996); [6] Horswill & Robinson (2015); [7] Gyimesi et al. (2011); [8] Camphuysen in Koffijberg et al. (2017); [9] Spaans et al. (1994); [10] Sellers & Shackleton (2011); [11] Perrins & Smith (2000); [12] Mavor et al. (2008); [13] Calladine & Harris (1997).

Herring gull

The population model for herring gull consists of a first-year stage (stage J0), three immature stages (I1 to I3), and an adult stage (A). Demographic rates and references are reported in Table 3.2.

Table 3.2 *Demographic rates of null model for herring gull. Si indicates the survival rate of stage* i. *Fecundity is presented as the number of fledglings per breeding pair. Prob. floater indicates the probability of non-breeding for an adult.*

	Mean	sd	Reference
SJ0	0.375	0.06	[1]; [2]; [3]
SI1	0.8	0.052	[1]; [4]
SI2	0.8	0.052	[1]; [4]
SI3	0.8	0.052	[1]; [4]
SA	0.8646	0.03	[2]; [3]; [4]; [5]
Fecundity	0.8532	0.2	[3]; [4]; [6]; [7]; [8]
Prob. floater	0.10	0.05	estimate

References: [1] Camphuysen (2013); [2] Chabrzyk & Coulson (1976); [3] Wanless et al. (1996); [4] Camphuysen & Gronert (2012); [5] Glutz von Blotzheim et al. (1984); [6] Camphuysen in Koffijberg et al. (2017); [7] Koffijberg et al. (2017); [8] Sellers & Shackleton (2011).

Great black-backed gull

The population model for great black-backed gull consists of a first-year stage (stage J0), three immature stages (I1 to I3), and an adult stage (A). Demographic rates and references are reported in Table 3.3.

Table 3.3 *Demographic rates of null model for great black-backed gull. Si indicates the survival rate of stage* i. *Fecundity is presented as the number of fledglings per breeding pair. Prob. floater indicates the probability of non-breeding for an adult.*

	Mean	sd	Reference
SJ0	0.34	0.05	[1]
SI1	0.8	0.03	[1]
SI2	0.8	0.03	[1]
SI3	0.8	0.03	[1]
SA	0.86	0.02	[2]; [3]
Fecundity	0.98	0.4	[4]; [5]; [6]; [7]
Prob. floater	0.10	0.05	[8]

References: [1] Collier et al. (2020); [2] Glutz von Blotzheim et al. (1984); [3] Barrett et al. (2015); [4] Mavor et al. (2008); [5] Verbeek (1979); [6] Schekkerman et al. (2017); [7] Butler & Trivelpiece (1981); [8] Robinson (2018).

Black-legged kittiwake

The population model for black-legged kittiwake consists of a first-year stage (stage J0), three immature stages (I1 to I3), and an adult stage (A). Demographic rates and references are reported in Table 3.4.

Table 3.4 *Demographic rates of null model for black-legged kittiwake. Si indicates the survival rate of stage* i. *Fecundity is presented as the number of fledglings per breeding pair. Prob. floater indicates the probability of non-breeding for an adult.*

	Mean	sd	Reference
SJ0	0.79	0.05	[1]; [2]
SI1	0.7	0.04	[1]; [3]; [13]; [14]; [15]
SI2	0.7	0.04	[1]; [3]; [13]; [14]; [15]
SI3	0.7	0.04	[1]; [3]; [13]; [14]; [15]
SA	0.854	0.05	[1] to [10]; [13] to [15]; [18] to [21]
Fecundity	0.66	0.2	[1]; [3]; [5]; [11]; [12]; [13] to [15]
Prob. floater	0.10	0.05	Estimate

References: [1] Coulson & White (1959); [2] Horswill & Robinson (2015); [3] Thomas & Coulson (1988); [4] Harris et al. (2000); [5] Frederiksen et al. (2004); [6] Cam et al. (2002); [7] Sandvik et al. (2005); [8] Coulson & Wooller (1976); [9] Reiertsen et al. (2014); [10] del Hoyo et al. (1996); [11] Mavor et al. (2008); [12] JNCC Seabird Monitoring Programme Database, www.jncc.gov.uk/smp; [13] Searle et al. (2020); [14] Freeman et al. (2014); [15] Jitlal et al. (2016); [16] Christensen-Dalsgaard et al. (2019); [17] Christensen-Dalsgaard et al. (2018) [18] Horswill et al. (2021); [19] Rothery et al. (2002); [20] Oro & Furness (2002); [21] Coulson & Strowger (1999).

Northern gannet

The population model for northern gannet consists of a first-year stage (stage J0), three immature stages (I1 to I3), and two adult stages (A4 and AB). Individuals in stage A4 (4 years old) have adult survival, but do not reproduce yet, while AB are adults which can reproduce. Demographic rates and references are reported in Table 3.5.

Table 3.5 *Demographic rates of null model for northern gannet. Si indicates the survival rate of stage* i. *Fecundity is presented as the number of fledglings per breeding pair. Prob. floater indicates the probability of non-breeding for an adult.*

	Mean	**sd**	**Reference**
SJ0	0.481	0.0853	
SI1	0.816	0.0393	
SI2	0.884	0.0293	
SI3	0.887	0.0301	
SA	0.918	0.0199	
Fecundity	0.7	0.082	[Searle et al. 2020]
Prob. floater	0.05	0.125	

References: [1] (Searle *et al.* 2019)

Arctic skua

The population model for arctic skua consists of a first-year stage (stage J0), three immature stages (I1 to I3), and an adult stage (A). Demographic rates and references are reported in Table 3.6.

Table 3.6 *Demographic rates of null model for Arctic skua. Si indicates the survival rate of stage* i. *Fecundity is presented as the number of fledglings per breeding pair. Prob. floater indicates the probability of non-breeding for an adult.*

	Mean	**sd**	**Reference**
SJ0	0.57	0.05	[1]; [2]; [3]; [16]
SI1	0.77	0.05	[1]; [4]
SI2	0.77	0.05	[1]; [4]
SI3	0.77	0.05	[1]; [4]
SA	0.9	0.05	[1]; [2]; [5]; [15]; [16]
Fecundity	0.488	0.1	[3]; [5] to [14]; [15]
Prob. floater	0.25	0.05	estimate

References: [1] O'Donald (1983); [2] Robinson (2018); [3] Cook & Robinson (2010); [4] Horswill & Robinson (2015); [5] Phillips & Furness (1998); [6] O'Donald et al. (1974); [7] Phillips et al. (1996); [8] Dawson et al. (2011); [9] Perkins et al. (2018); [10] Mavor et al. (2008); [11] Jones (2003); [12] Baber (1989); [13] Baber (1990); [14] Furness & Aitken (1992); [15] Van Bemmelen et al. (2021); [16] Snell (pers. comm.).

Great skua

The population model for great skua consists of a first-year stage (stage J0), six immature stages (I1 to I6), and an adult stage (A). Demographic rates and references are reported in Table 3.7.

Table 3.7 *Demographic rates of null model for great skua. Si indicates the survival rate of stage* i. *Fecundity is presented as the number of fledglings per breeding pair. Prob. floater indicates the probability of non-breeding for an adult.*

	Mean	sd	Reference
SJ0	0.97	0.05	[1] to [3]
SI1	0.78	0.05	[4]
SI2	0.78	0.05	[4]
SI3	0.78	0.05	[4]
SI4	0.78	0.05	[4]
SI5	0.78	0.05	[4]
SI6	0.78	0.05	[4]
SA	0.882	0.055	[1] to [8]
Fecundity	0.536	0.3	[7]; [9] to [12]
Prob. floater	0.089	0.01	[7]

References: [1] Machado dos Santos (2018); [2]. Snell (pers. comm.); [3] Collier et al (2020); [4] Furness (1978); [5] Balmer & Peach (1997); [6] Ratcliffe et al. (2002); [7] Catry et al. (1998); [8] del Hoyo et al. (1996); [9] JNCC Seabird Monitoring Programme Database, www.jncc.gov.uk/smp; Fair Isle; [10] Jones et al. (2008); [11] Phillips et al. (1999); [12] Mavor et al. (2008); [13] Robinson (2018); [14] Horswill & Robinson (2015).

Common tern

The population model for common tern consists of a first-year stage (stage J0), three immature stages (I1 to I3), and an adult stage (A). Demographic rates and references are reported in Table 3.8.

Table 3.8 *Demographic rates of null model for common tern. Si indicates the survival rate of stage* i. *Fecundity is presented as the number of fledglings per breeding pair. Prob. floater indicates the probability of non-breeding for an adult.*

	Mean	sd	Reference
SJ0	0.685	0.05	[1]
SI1	0.72	0.05	[1] to [4]
SI2	0.72	0.05	[1] to [4]
SI3	0.72	0.05	[1] to [4]
SA	0.915	0.05	[1] to [4]
Fecundity	0.646	0.2	[1]; [3] to [17]
Prob. floater	0.1	0.03	estimate

References: [1] Van der Jeugd *et al.* (2014); [2] Becker and Ludwigs (2004); [3] Becker *et al.* (2001); [4] Schekkerman *et al*. (2021); [5] Schekkerman *et al*. (2017); [6] Stienen *et al*. (2009), based on reports Griend study area; [7] Becker *et al*. (1994); [8] JNCC (2020); [9] Becker (1998); [10] van der Winden *et al*. (2018); [11] van der Winden *et al*. (2019a); [12] Thorup and Koffijberg (2015); [13] Becker (1998); [14] Walsh *et al*. (1991); [15] Zintl (1998); [16] Koffijberg *et al*. (2017); [17] van der Winden *et al*. (2019b).

Sandwich tern

The population model for sandwich tern consists of a first-year stage (stage J0), an immature stage lasting two years (I1 and I2) and an two adult stages (A3 and AB). Individuals in stage A3 can reproduce, but with lower fecundity than older adults (AB, from age 4 onwards). Survival in stage A3 is assumed to be the same as in stage AB (adult survival). Demographic rates and references are reported in Table 3.9.

Table 3.9 *Demographic rates of null model for sandwich tern. Si indicates the survival rate of stage* i. *Fecundity is presented as the number of fledglings per breeding pair. *: fecundity during third calendar year is lower due to lack of experience. Standard deviation is applied to the fecundity of 0.325, after which the correction factor of 0.3 is applied. Prob. floater indicates the probability of non-breeding for an adult.*

	Mean	sd	Reference
SJ0	0.508	0.0917	
SI1	0.777	0.0518	
SA	0.942	0.108	
Fecundity age 3	0.3 x 0.325	*	
Fecundity from age 4 onwards	0.325	0.160	
Prob. floater	0.1	0.125	

Bewick's swan

The population model for Bewick's swan consists of a first-year stage (stage J0), one immature stage (I1) and an adult stage (A). Demographic rates and references are reported in Table 3.10. For this species, fecundity is based on relative numbers of firstyear individuals and adults. Floaters are included in this estimate for fecundity, and are therefore not separately taken into account in the population model.

Table 3.10 *Demographic rates of null model for Bewick's swan. Si indicates the survival rate of stage* i. *Fecundity is presented as the number of fledglings per adult, divided by two. For this species, fecundity is based on relative numbers of firstyear individuals and adults. Floaters are included in this estimate for fecundity, and are therefore not separately taken into account in the population model.*

	Mean	sd	Reference
SJ0	0.908	0.05	[1]
SI1	0.936	0.05	[1]
SA	0.873	0.05	[1]
Fecundity	0.278	0.1	Based on [1], adjusted for first six months survival
Prob. floater	-	-	-

References: [1] Nuijten *et al.* (2020).

Brent goose

The population model for brent goose consists of a first-year stage (stage J0), one immature stage (I1) and an adult stage (A). Demographic rates and references are reported in Table 3.11. For this species, fecundity is based on relative numbers of firstyear individuals and adults. Floaters are included in this estimate for fecundity, and are therefore not separately taken into account in the population model.

Table 3.11 *Demographic rates of null model for brent goose. Si indicates the survival rate of stage* i. *Fecundity is presented as the number of fledglings per adult, divided by two. For this species, fecundity is based on relative numbers of firstyear individuals and adults. Floaters are included in this estimate for fecundity, and are therefore not separately taken into account in the population model.*

	Mean	sd	Reference
SJ0	0.51	0.05	[1]
SI1	0.849	0.05	[1]; [3] to [5]
SA	0.868	0.03	[1] to [3]; [6] to [8]; [13]
Fecundity	0.588	0.1	[9]
Prob. floater	-	-	-

References: [1] Sedinger et al. (2007); [2] Robinson (2018); [3] Ebbinge et al. (2002); [4] Boyd (1962); [5] Balmer & Peach (1997); [6] Sedinger et al. (2002); [7] Cramp (1986); [8] Desholm (2009); [9] Nolet et al. (2013); [10] Nicolai (2003), Chapter 2; [11] WWT monitoring programme; https://monitoring.wwt.org.uk/our-work/goose-swan-monitoring-programme/species-accounts/dark-bellied-brent-goose; [12] Sedinger et al. (2006); [13] Cleasby et al. (2017).

Common shelduck

The population model for shelduck consists of a first-year stage (stage J0), one immature stage (I1) and an adult stage (A). Demographic rates and references are reported in Table 3.12.

Table 3.12 *Demographic rates of null model for common shelduck. Si indicates the survival rate of stage* i. *Fecundity is presented as the number of fledglings per breeding pair. Prob. floater indicates the probability of non-breeding for an adult.*

	Mean	sd	Reference
SJ0	0.25	0.05	[1]; [2]
SI1	0.67	0.05	[1]; [2]
SA	0.873	0.05	[1] to [3]
Fecundity	3.7	0.1	[4]
Prob. floater	0.35	0.05	estimate, based on [4] and validation with observed trend

References: [1] Patterson et al. (1983); [2] Robinson (2018); [3] Pienkowski & Evans (1982); [4] Lensink (2001).

Curlew

The population model for curlew consists of a first-year stage (stage J0), one immature stage (I1) and an adult stage (A). Demographic rates and references are reported in Table 3.13.

Table 3.13 *Demographic rates of null model for curlew. Si indicates the survival rate of stage i. Fecundity is presented as the number of fledglings per breeding pair. Prob. floater indicates the probability of non-breeding for an adult. *: validated with observed population trend*

	Mean	**sd**	**Reference**
SJ0	0.5595	0.05	[1]; [2]
SI1	0.771	0.05	[1]; [2]
SA	0.912	0.05	[1]; [2]
Fecundity	0.34	0.1	[3]
Prob. floater	0.1	0.05	Estimate *

References: [1] Collier et al. (2020); [2] Gerritsen (2001); [3] Roodbergen et al. (2012).

Red knot

The population model for red knot consists of a first-year stage (stage J0), one immature stage (I1) and an adult stage (A). Demographic rates and references are reported in Table 3.14.

Table 3.14 *Demographic rates of null model for red knot. Si indicates the survival rate of stage i. Fecundity is presented as the number of fledglings per breeding pair. Prob. floater indicates the probability of non-breeding for an adult. *: validated with observed population trend*

	Mean	**sd**	**Reference**
SJ0	0.782	0.03	[1]; [2]
SI1	0.842	0.01	[2] to [4]
SA	0.842	0.01	[2] to [4]
Fecundity	0.284	0.03	[5]
Prob. floater	0.1	0.03	Estimate *

References: [1] Leyrer et al. (2013); [2] Spaans et al. (2011); [3] Brochard et al. (2002); [4] Rakhimberdiev et al. 2015; [5] Meltofte (2008).

Bar-tailed godwit

The population model for bar-tailed godwit consists of a first-year stage (stage J0), one immature stage (I1) and an adult stage (A). Demographic rates and references are reported in Table 3.15.

Table 3.15 *Demographic rates of null model for bar-tailed godwit. Si indicates the survival rate of stage* i. *Fecundity is presented as the number of fledglings per breeding pair. Prob. floater indicates the probability of non-breeding for an adult. *: validated with observed population trend*

	Mean	sd	Reference
SJ0	0.57	0.05	[1]
SI1	0.8275	0.02	[1]; [2]
SA	0.8275	0.02	[1]; [2]
Fecundity	0.8	0.03	Estimate *
Prob. floater	0.1	0.05	Estimate *

References: [1] Spaans et al. (2011); [2] Piersma et al. (2015).

Black tern

The population model for black tern consists of a first-year stage (stage J0), two immature stage (I1 and I2) and an adult stage (A). Demographic rates and references are reported in Table 3.16. Reproduction occurs in stage I2 and the adult stage, with a higher probability of floaters in the I2 stage.

Table 3.16 *Demographic rates of null model for black tern. Si indicates the survival rate of stage* i. *Fecundity is presented as the number of fledglings per breeding pair. Prob. floater indicates the probability of non-breeding for an adult.*

	Mean	sd	Reference
SJ0	0.595	0.05	[1]
SI1	0.595	0.05	[1]
SI2	0.595	0.05	[1]
SA	0.846	0.05	[1]; [5]
Fecundity	0.93	0.1	[1] to [4]
Prob. floater I2 stage	0.8	0.05	estimate
Prob. floater adult stage	0.1	0.05	estimate

References: [1] van der Winden & Horssen (2008); [2] Tinbergen & Heemskerk (2016); [3] van der Winden (2008); [4] van der Winden (2005); [5] van den Winden & van Horssen, unpublished data.

Common starling

The population model for common starling consists of a first-year stage (stage J0) and an adult stage (A). Demographic rates and references are reported in Table 3.17. For this species, no floaters are assumed.

Table 3.17 *Demographic rates of null model for common starling. Si indicates the survival rate of stage* i. *Fecundity is presented as the number of fledglings per breeding pair. For this species, we assumed no floaters.*

	Mean	sd	Reference
SJ0	0.102	0.034	[1]; [2]
SA	0.607	0.151	[1]; [2]
Fecundity	4.43	0.075	[1]; [2]
Prob. floater	-	-	-

References: [1] Versluijs et al. (2016); [2] Schippers et al. (2020).

3.2 Apportionment of victims among stages

Certain age classes could be more impacted than others. For the apportionment of victims between age classes, we assumed that the age distribution at sea is an indication for the age distribution among victims. In this chapter we provide the apportionments used in the calculations.

If certain age classes suffer higher collision risk due to more time spent offshore, the survival rates of these stages are adjusted more strongly than for other stages that do not spend much time offshore. If available, data from age distributions at sea are used as indicator for time spent offshore, for example based on the analysis within Potiek *et al.* (2019b). If based on Potiek *et al.* (2019b), the overall annual stage distribution in the entire southern North Sea is used, without taking into account spatial- and/or temporal variation.

For each species, we present a table with the following information for each life stage:

- *life stages:* survival rates can be applied to several stages, for example when several immature stages have the same survival rate.
- *stable stage distribution*: overall stage distribution in the population. If all age classes have the same vulnerability, the stage distribution among victims is assumed to be the same as the stable stage distribution.
- *vulnerability:* this represents the relative collision vulnerability of each age class. The vulnerability is 1 for the stage with the highest relative vulnerability. If no data are available for stage-specific differences in vulnerability, each stage has a vulnerability of 1, and the stage distribution among victims is assumed to follow the stable stage distribution. If a stage is not present in the southern North Sea, the vulnerability of this stage is 0, and if a species is present during six months, this is 0.5. If data are available on the age distribution at sea, for example based on ESAS/MWTL data, the vulnerability is assumed to follow this age distribution. If one survival rate applies to several stages, the vulnerability vector has several values as well, corresponding to each of the life stages.
- *scalar*: the scalar is the factor with which the survival is adjusted. As a result of multiplication with this stage-specific scalar, the stage distribution among victims

is adjusted to follow the distribution as given in the vulnerability vector. Although the vulnerability vector can apply to several stages, the scalar is specific for each survival rate. This means that immature survival is adjusted with one specific scalar, even if several stages experience this survival rate.

Lesser black-backed gull

Victims were apportioned among age classes according to Camphuysen and Leopold (1994). The authors analysed the age distribution in the southern North Sea, and showed that 82.9% of all individuals were adults, 10.3% were first-year individuals, and the remaining 6.8% were immatures. We assumed the same age distribution among victims.

Table 3.18 *Apportionment of victims among life stages for lesser black-backed gull. For each survival parameter, the relevant life stages are reported, and the stable stage distribution within the population. The vulnerability presents the relative vulnerability of individuals per age class (highest vulnerability is 1), which is presented for each life stage (hence several values). OWF scalar is used to adjust the mortality fraction for each survival rate, in order to match the relative stage structure among victims with OWF vulnerability.*

Survival parameter	Life Stage	Stable stage distribution	Relative OWF vulnerability	OWF scalar
SJ0	J0	0.07011	0.12	0.18290
SI	I1,I2,I3,I4	0.26472	0.02,0.02,0.02,0.02	0.03019
SA	A	0.66517	1	1.47208

Herring gull

Individuals spending more time at sea are assumed to experience higher collision risk. Therefore, we used data from Camphuysen & Leopold (1994) to assess the distribution of age classes at sea. Based on this data source, we assumed 67% adults, 14% immatures, and 19% first-year individuals. This results in a stage-specific additional annual mortality.

Table 3.19 *Apportionment of victims among life stages for herring gull. For each survival parameter, the relevant life stages are reported, and the stable stage distribution within the population. The vulnerability presents the relative vulnerability of individuals per age class (highest vulnerability is 1), which is presented for each life stage (hence several values). OWF scalar is used to adjust the mortality fraction for each survival rate, in order to match the relative stage structure among victims with OWF vulnerability.*

Survival parameter	Life Stage	Stable stage distribution	Relative OWF vulnerability	OWF scalar
SJ0	J0	0.10844	0.28	0.41029
SI1	I1	0.09742	0.07	0.10078
SI2	I2	0.08200	0.07	0.10078
SI3	I3	0.06902	0.07	0.10078
SA	A	0.64312	1	1.44681

Little gull

For little gull, data from Potiek *et al.* (2019) have been used. This analysis of ESAS data showed that 87% of all individuals with assigned age distribution during the ESAS surveys were adults. The summed relative vulnerability of other stages is the remaining 13%, which is divided among the J0 and immature stages based on the stable stage distribution.

Table 3.20 Apportionment of victims among life stages for little gull. For each survival parameter, the relevant life stages are reported, and the stable stage distribution within the population. The vulnerability presents the relative vulnerability of individuals per age class (highest vulnerability is 1), which is presented for each life stage (hence several values). OWF scalar is used to adjust the mortality fraction for each survival rate, in order to match the relative stage structure among victims with OWF vulnerability.

Survival parameter	Life Stage	Stable stage distribution	Relative OWF vulnerability	OWF scalar
SJ0	J0	0.10651	0.06	0.07777
SI	I1	0.17687	0.09	0.12443
SA	A	0.71661	1	1.35318

Great black-backed gull

For great black-backed gull, the stage distribution is based on ESAS data (analysed by Potiek *et al.*, 2019). This analysis of ESAS data showed that 58% of all individuals with assigned age distribution during the ESAS surveys were adults. The summed relative vulnerability of other stages is the remaining 42%, which is divided among the J0 and immature stages based on the stable stage distribution.

Table 3.21 Apportionment of victims among life stages for great black-backed gull. For each survival parameter, the relevant life stages are reported, and the stable stage distribution within the population. The vulnerability presents the relative vulnerability of individuals per age class (highest vulnerability is 1), which is presented for each life stage (hence several values). OWF scalar is used to adjust the mortality fraction for each survival rate, in order to match the relative stage structure among victims with OWF vulnerability.

Survival parameter	Life Stage	Stable stage distribution	Relative OWF vulnerability	OWF scalar
SJ0	J0	0.11958	1	1.57546
SI	I1,I2,I3	0.25287	1, 0.93, 0.95	1.51825
SA	A	0.62755	0.43	0.68152

Black-legged kittiwake

For black-legged kittiwake, the stage distribution is based on ESAS data (analysed by Potiek *et al.*, 2019). This analysis of ESAS data showed that 88% of all individuals with assigned age distribution during the ESAS surveys were adults. The summed relative vulnerability of other stages is the remaining 12%, which is divided among the J0 and immature stages based on the stable stage distribution.

Table 3.22 Apportionment of victims among life stages for black-legged kittiwake. For each survival parameter, the relevant life stages are reported, and the stable stage distribution within the population. The vulnerability presents the relative vulnerability of individuals per age class (highest vulnerability is 1), which is presented for each life stage (hence several values). OWF scalar is used to adjust the mortality fraction for each survival rate, in order to match the relative stage structure among victims with OWF vulnerability.

Survival parameter	Life Stage	Stable stage distribution	Relative OWF vulnerability	OWF scalar
SJ0	J0	0.07976	0.03	0.04907
SI	I1,I2,I3	0.33216	0.03,0.04,0.03	0.05835
SA	A	0.58808	1	1.66083

Northern gannet

For northern gannet, the stage distribution is based on ESAS data (analysed by Potiek *et al.*, 2019). This analysis of ESAS data showed that 73% of all individuals with assigned age distribution during the ESAS surveys were adults. Stages I1 to I3 are not present on the North Sea, and are therefore not vulnerable for collision with OWFs in this area. The summed relative vulnerability of other stages is the remaining 27%, which is divided among the J0 and A4 stages based on the stable stage distribution.

Table 3.23 Apportionment of victims among life stages for northern gannet. For each survival parameter, the relevant life stages are reported, and the stable stage distribution within the population. The vulnerability presents the relative vulnerability of individuals per age class (highest vulnerability is 1), which is presented for each life stage (hence several values). OWF scalar is used to adjust the mortality fraction for each survival rate, in order to match the relative stage structure among victims with OWF vulnerability.

Survival parameter	Life Stage	Stable stage distribution	Relative OWF vulnerability	OWF scalar
SJ0	J0	0.09082	0.22	0.34470
S1	I1	0.09623	0	0.00000
S2	I2	0.07784	0	0.00000
S3	I3	0.06822	0	0.00000
SA	A4,AB	0.66690	0.15,1	1.45254

Arctic skua

For arctic skua, the stage distribution is based on ESAS data (analysed by Potiek *et al.*, 2019). This analysis of ESAS data showed that 63% of all individuals with assigned age distribution during the ESAS surveys were adults. The summed relative vulnerability of other stages was the remaining 37%, divided among the subadult stages based on the stable stage distribution.

Table 3.24 *Apportionment of victims among life stages for arctic skua. For each survival parameter, the relevant life stages are reported, and the stable stage distribution within the population. The vulnerability presents the relative vulnerability of individuals per age class (highest vulnerability is 1), which is presented for each life stage (hence several values). OWF scalar is used to adjust the mortality fraction for each survival rate, in order to match the relative stage structure among victims with OWF vulnerability.*

Survival parameter	Life Stage	Stable stage distribution	Relative OWF vulnerability	OWF scalar
SJ0	J0	0.06304	0.12	0.15332
SI	I1,I2,I3	0.19829	0.12,0.19,0.16	0.19664
SA	A	0.73867	1	1.28791

Great skua

For great skua, the stage distribution is based on ESAS data (analysed by Potiek *et al.*, 2019). This analysis of ESAS data showed that 82% of all individuals with assigned age distribution during the ESAS surveys were adults. The summed relative vulnerability of other stages was the remaining 18%, divided among the subadult stages based on the stable stage distribution.

Table 3.25 *Apportionment of victims among life stages for great skua. For each survival parameter, the relevant life stages are reported, and the stable stage distribution within the population. The vulnerability presents the relative vulnerability of individuals per age class (highest vulnerability is 1), which is presented for each life stage (hence several values). OWF scalar is used to adjust the mortality fraction for each survival rate, in order to match the relative stage structure among victims with OWF vulnerability.*

Survival parameter	Life Stage	Stable stage distribution	Relative OWF vulnerability	OWF scalar
SJ0	J0	0.05546	0.03	0.05615
SI	I1,I2,I3, I4,I5,I6	0.46190	0.03,0.05,0.04, 0.03,0.03,0.02	0.06643
SA	A	0.48264	1	2.00189

Common tern

For common tern, the stage distribution is based on ESAS data (analysed by Potiek *et al.*, 2019). This analysis of ESAS data showed that 89% of all individuals with assigned age distribution during the ESAS surveys were adults. The summed relative vulnerability of other stages was the remaining 11%, divided among the subadult stages based on the stable stage distribution.

Table 3.26 *Apportionment of victims among life stages for common tern. For each survival parameter, the relevant life stages are reported, and the stable stage distribution within the population. The vulnerability presents the relative vulnerability of individuals per age class (highest vulnerability is 1), which is presented for each life stage (hence several values). OWF scalar is used to adjust the mortality fraction for each survival rate, in order to match the relative stage structure among victims with OWF vulnerability.*

Survival parameter	Life Stage	Stable stage distribution	Relative OWF vulnerability	OWF scalar
SJ0	J0	0.08337	0.03	0.05433
SI	I1,I2,I3	0.28567	0,0.05,0.04	0.03952
SA	A	0.63096	1	1.55981

Sandwich tern

For sandwich tern, victims were apportioned between life stages according to the stable stage structure based on the population models. This means that individuals from different age classes have the same collision probability. However, in case of sandwich tern, only adults are assumed to be vulnerable for collision. For that reason, the vulnerability of the J0 and I1 stage is 0.

Table 3.27 *Apportionment of victims among life stages for sandwich tern. For each survival parameter, the relevant life stages are reported, and the stable stage distribution within the population. The vulnerability presents the relative vulnerability of individuals per age class (highest vulnerability is 1), which is presented for each life stage (hence several values). OWF scalar is used to adjust the mortality fraction for each survival rate, in order to match the relative stage structure among victims with OWF vulnerability.*

Survival parameter	Life Stage	Stable stage distribution	Relative OWF vulnerability	OWF scalar
SJ0	1	J0	0	0
SI	2	I1	0	0
SA	3	A3,AB	1, 1	1

Bewick's swan

For Bewick's swan, victims were apportioned between life stages according to a stable stage structure based on the population models. This means that individuals from different age classes have the same collision probability.

Table 3.28 *Apportionment of victims among life stages for Bewick's swan. For each survival parameter, the relevant life stages are reported, and the stable stage distribution within the population. The vulnerability presents the relative vulnerability of individuals per age class (highest vulnerability is 1), which is presented for each life stage (hence several values). OWF scalar is used to adjust the mortality fraction for each survival rate, in order to match the relative stage structure among victims with OWF vulnerability.*

Survival parameter	Life Stage	Stable stage distribution	Relative OWF vulnerability	OWF scalar
SJ0	J0	0.05491	1	1
SI	I1	0.10670	1	1
SA	A	0.83839	1	1

Brent goose

For brent goose, victims were apportioned between life stages according to a stable stage structure. This means that individuals from different age classes have the same collision probability.

Table 3.29 *Apportionment of victims among life stages for brent goose. For each survival parameter, the relevant life stages are reported, and the stable stage distribution within the population. The vulnerability presents the relative vulnerability of individuals per age class (highest vulnerability is 1), which is presented for each life stage (hence several values). OWF scalar is used to adjust the mortality fraction for each survival rate, in order to match the relative stage structure among victims with OWF vulnerability.*

Survival parameter	Life Stage	Stable stage distribution	Relative OWF vulnerability	OWF scalar
SJ0	J0	0.10177	1	1
SI	I1	0.11756	1	1
SA	A	0.78068	1	1

Common shelduck

Common shelducks from their second calendar year onwards (Wernham *et al.*, 2002). Individuals in stage J0 are therefore not vulnerable for collisions with wind farms on the North Sea. The vulnerability of immatures and adults is assumed to be equal.

Table 3.30 Apportionment of victims among life stages for common shelduck. For each survival parameter, the relevant life stages are reported, and the stable stage distribution within the population. The vulnerability presents the relative vulnerability of individuals per age class (highest vulnerability is 1), which is presented for each life stage (hence several values). OWF scalar is used to adjust the mortality fraction for each survival rate, in order to match the relative stage structure among victims with OWF vulnerability.

Survival parameter	Life Stage	Stable stage distribution	Relative OWF vulnerability	OWF scalar
SJ0	J0	0.24191	0	0.00000
SI	I1	0.16718	1	1.00000
SA	A	0.59091	1	1.00000

Eurasian curlew

For curlew, victims were apportioned between life stages according to a stable stage structure. This means that individuals from different age classes have the same collision probability.

Table 3.31 Apportionment of victims among life stages for Eurasian curlew. For each survival parameter, the relevant life stages are reported, and the stable stage distribution within the population. The vulnerability presents the relative vulnerability of individuals per age class (highest vulnerability is 1), which is presented for each life stage (hence several values). OWF scalar is used to adjust the mortality fraction for each survival rate, in order to match the relative stage structure among victims with OWF vulnerability.

Survival parameter	Life Stage	Stable stage distribution	Relative OWF vulnerability	OWF scalar
SJ0	J0	0.06167	1	1
SI	I1	0.07542	1	1
SA	A	0.86290	1	1

Black tern

For black tern, the stage distribution is based on ESAS data (analysed by Potiek *et al.*, 2019). This analysis of ESAS data showed that 82% of all individuals with assigned age distribution during the ESAS surveys were adults. The summed relative vulnerability of other stages was the remaining 18%. As only the stage J0 and I2 make use of the North Sea, this 18% is divided among these stages based on the stable stage distribution.

Table 3.32 *Apportionment of victims among life stages for black tern. For each survival parameter, the relevant life stages are reported, and the stable stage distribution within the population. The vulnerability presents the relative vulnerability of individuals per age class (highest vulnerability is 1), which is presented for each life stage (hence several values). OWF scalar is used to adjust the mortality fraction for each survival rate, in order to match the relative stage structure among victims with OWF vulnerability.*

Survival parameter	Life Stage	Stable stage distribution	Relative OWF vulnerability	OWF scalar
SJ0	J0	0.11564	0.23	0.34200
SI	I1,I2	0.27187	0,0.29	0.16508
SA	A	0.61249	1	1.49484

Common starling

For common starling, victims were apportioned between life stages according to a stable stage structure. This means that individuals from different age classes have the same collision probability.

Table 3.33 *Apportionment of victims among life stages for common starling. For each survival parameter, the relevant life stages are reported, and the stable stage distribution within the population. The vulnerability presents the relative vulnerability of individuals per age class (highest vulnerability is 1), which is presented for each life stage (hence several values). OWF scalar is used to adjust the mortality fraction for each survival rate, in order to match the relative stage structure among victims with OWF vulnerability.*

Survival parameter	Life Stage	Stable stage distribution	Relative OWF vulnerability	OWF scalar
SJ0	J0	0.3434	1	1
SA	A	0.6566	1	1

Bar-tailed godwit

Bar-tailed godwits generally spend the summer of their second calendar-year in wintering grounds. This means that individuals are vulnerable for collision during migration towards wintering grounds in their first autumn, and from the spring migration during their third calendar-year onwards. In addition, victims were apportioned according to a stable stage structure. This means that individuals making use of the North Sea have the same collision probability.

Table 3.34 Apportionment of victims among life stages for bar-tailed godwit. For each survival parameter, the relevant life stages are reported, and the stable stage distribution within the population. The vulnerability presents the relative vulnerability of individuals per age class (highest vulnerability is 1), which is presented for each life stage (hence several values). OWF scalar is used to adjust the mortality fraction for each survival rate, in order to match the relative stage structure among victims with OWF vulnerability.

Survival parameter	Life Stage	Stable stage distribution	Relative OWF vulnerability	OWF scalar
SJ0	J0	0.11497	0.5	0.57668
SI	I1	0.15098	0.5	0.57668
SA	A	0.73406	1	1.15336

Red knot

For red knot, victims were apportioned between life stages according to a stable stage structure. This means that individuals from different age classes have the same collision probability.

Table 3.35 Apportionment of victims among life stages for red knot. For each survival parameter, the relevant life stages are reported, and the stable stage distribution within the population. The vulnerability presents the relative vulnerability of individuals per age class (highest vulnerability is 1), which is presented for each life stage (hence several values). OWF scalar is used to adjust the mortality fraction for each survival rate, in order to match the relative stage structure among victims with OWF vulnerability.

Survival parameter	Life Stage	Stable stage distribution	Relative OWF vulnerability	OWF scalar
SJ0	J0	0.05174	1	1
SI	I1	0.09181	1	1
SA	A	0.85645	1	1

4 Victims per wind farm scenario

In this chapter, we provide the results of the sCRM calculations and how these figures translate to mortality fractions relative to the used population sizes, first for seabirds (§4.1) and then for migratory birds (§4.2).

4.1 Seabirds

Table 4.1 *Numbers of estimated annual victims per scenario for seabirds. The population size is defined as the maximum bimonthly number of individuals present.*

	'Population' size		Number of victims per scenario				
Species	Dutch continental plate (national)	Southern North Sea (international)	Basic nat 30	Rekenvariant III	Rekenvariant II	Rekenvariant I	Int 30
Lesser black-backed gull	20,553	75,351	97 ± 5	153 ± 7	144 ± 7	139 ± 7	441 ± 10
Herring gull	21,138	124,964	180 ± 12	236 ± 13	223 ± 13	219 ± 13	655 ± 27
Little gull	57,833	55,817	91 ± 2	117 ± 2	112 ± 2	110 ± 2	143 ± 2
Great black-backed gull	16,264	92,417	338 ± 26	666 ± 48	578 ± 41	550 ± 41	2,174 ± 73
Black-legged kittiwake	78,921	444,163	229 ± 3	425 ± 5	381 ± 5	364 ± 5	1,268 ± 55
Northern gannet	31,858	162,867	1,183 ± 49	1,925 ± 66	1,771 ± 63	1,690 ± 62	7,001 ± 126
Arctic skua	130	3,186	0.07 ± 0.01	0.09 ± 0.01	0.09 ± 0.01	0.09 ± 0.01	1.89 ± 0.03
Great skua	1,364	12,103	2 ± 0.2	6 ± 0.8	5 ± 0.8	5 ± 0.8	29 ± 1.7
Common tern	59,093	74,947	43 ± 2	58 ± 2	56 ± 2	55 ± 2	99 ± 2
Sandwich tern	22,602	25,881	32 ± 0.7	41 ± 0.8	40 ± 0.8	40 ±0.8	65 ± 0.9

Table 4.2 Mortality fraction per scenario for seabirds.

Species	Mortality fraction = 1 – (1- mean bimonthly mortality) ^ 6 / ‘Population’				
	Basic nat 30	Rekenvariant III	Rekenvariant II	Rekenvariant I	Int 30
Lesser black-backed gull	0.00470	0.00743	0.00701	0.00675	0.00584
Herring gull	0.00848	0.01109	0.01052	0.01031	0.00523
Little gull	0.00157	0.00202	0.00194	0.00191	0.00254
Great black-backed gull	0.02063	0.04028	0.03500	0.03337	0.02330
Black-legged kittiwake	0.00290	0.00537	0.00482	0.00460	0.00285
Northern gannet	0.03657	0.05893	0.05432	0.05189	0.04223
Arctic skua	0.00056	0.00068	0.00068	0.00066	0.00059
Great skua	0.00148	0.00425	0.00376	0.00345	0.00241
Common tern	0.00073	0.00098	0.00094	0.00093	0.00132
Sandwich tern	0.00142	0.00183	0.00176	0.00176	0.00249

4.2 Migratory birds

Table 4.3 Numbers of estimated annual victims per scenario for migratory species.

		Number of victims per scenario				
Species	Autumn flux	Basic nat 30	Rekenvariant III	Rekenvariant II	Rekenvariant I	Int 30
Bewick's swan	17,450	3 ± 0.02	5 ± 0.03	5 ± 0.03	4 ± 0.03	10 ± 0.04
Brent goose	247,286	26 ± 0.06	51 ± 0.11	49 ± 0.11	44 ± 0.10	104 ± 0.13
Common shelduck	302,047	64 ± 2	128 ± 3	114 ± 3	106 ± 3	473 ± 5
Eurasian curlew	302,273	91 ± 2	182 ± 3	161 ± 3	151 ± 3	670 ± 5
Black tern	285,482	9 ± 0.1	18 ± 0.2	16 ± 0.1	15 ± 0.1	33 ± 0.2
Common starling	18,501,266	3,022 ± 15	6,154 ± 26	5,437 ± 24	5,078 ± 23	22,411 ± 41
Red knot	672,197	168 ± 0.3	341 ± 0.5	302 ± 0.4	282 ± 0.4	1245 ± 0.7
Bar-tailed godwit	347,670	98 ± 1	199 ± 2	176 ± 2	164 ± 2	729 ± 3

Table 4.4 Numbers of estimated annual victims per scenario for migratory species.

	Mortality Fraction (= myear / N)				
Species	Basic nat 30	Rekenvariant III	Rekenvariant II	Rekenvariant I	Int 30
Bewick's swan	0.00013	0.00026	0.00024	0.00022	0.00054
Brent goose	0.00010	0.00020	0.00020	0.00018	0.00042
Common shelduck	0.00021	0.00042	0.00038	0.00035	0.00157
Eurasian curlew	0.00030	0.00060	0.00053	0.00050	0.00221
Black tern	0.00003	0.00006	0.00006	0.00005	0.00012
Common starling	0.00016	0.00033	0.00029	0.00027	0.00121
Red knot	0.00025	0.00051	0.00045	0.00042	0.00185
Bar-tailed godwit	0.00028	0.00057	0.00051	0.00047	0.00210

5 Population-level impacts

The mortality estimates and the subsequent population model outcomes provided the basis for the evaluation of the population-level impacts. For these purposes the generated results were compared with the species-specific Acceptable Levels of Impact (ALI), as defined by the Ministry of Agriculture, Nature and Food Quality.

The ALI consists of two parts:

1. Maximally acceptable population decline (X). A threshold population decline 30 years after the impact, as a percentage X of the projected population size without the impact, which is considered ‘acceptable’. This decline that may already be violated in part of the unimpacted scenarios, as a result of the uncertainty in the population model. For that reason, the ALI consists also of a second part:
2. Maximally acceptable probability of the decline (Y), which is based on the chosen level of causality. With this level of causality, the probability of violating the X-threshold as result of the impact is calculated (i.e., not as the result of uncertainty in the population model).

Together, X and Y lead to an ALI, expressed as *‘The probability of a population decline of X% or more, 30 years after the onset of a continuous prolonged impact, cannot exceed Y’*.

In the following chapters, the outcome of this comparison is denoted by TRUE: the ALI threshold *is violated* or FALSE: the ALI threshold is *not violated*. In §5.1 the species-specific tables are presented and in §5.2 a summary of the assessments is provided in table 5.17.

For each species, this section consists of one table and two figures.

- *Table summarizing the results*: For each scenario, the bird abundance and the number of casualties result in the reported mortality fraction. In addition, the median population growth rate is reported, as well as the 5th and 95th percentile, which gives an indication of the range of projected population growth rates. The last two columns present the results of the comparison with the ALI threshold. ‘P causality’ represents the probability that a violation of the X threshold results from an OWF induced impact. The last column shows whether P causality violates the ALI threshold.
- *Figure presenting distribution of projected population growth rates for each scenario*. Each panel presents a different scenario. Within each panel the distribution of the unimpacted population growth rate (grey bars) is compared with the distribution of the impacted population growth rate (coloured bars). Black vertical lines indicate median population growth rates for the unimpacted scenario and red vertical lines indicate the threshold population growth rate (first part of the ALI, X% decline within 3 generations or 10 years). For each impacted scenario, different coloured vertical lines indicate the median. The larger the effect of the impact, the further the distribution of population growth rates moves towards the left. This shift results from a certain impact onwards in the median of the impacted

scenario getting below the median of the threshold scenario. This can be observed in the figures as the coloured vertical line (median of impacted scenario) being below the red vertical line (median of threshold). As mentioned earlier in this chapter, the ALI threshold is violated when the causality of ending up below the red line (i.e., violating the X threshold) as result of the impact exceeds the probability Y. Note that the ALI thresholds are species-specific. As result of differences in acceptable causality between two species, these figures should not be compared between species, but only between scenarios for a certain species. A higher acceptable causality means that the threshold is only violated when relatively more simulations violate the X-threshold, thus when the population growth rate distributions of the impacted and null scenarios are further apart.

- *The last figure shows the sensitivity analysis.* Each panel within the figure presents the sensitivity of individual demographic rates, as indicated in the title of each panel. On the vertical axis, the modelled population growth rate is reported following the changes in the tested parameter. The x-axis, with values varying between 0 and 1, indicates changes in the tested parameter. Note that these values do not necessarily resemble a realistic range. The sensitivity analysis is presented for each stage-specific survival, breeding success (number of fledglings per breeding pair) and probability of floaters. A steeper trend indicates a stronger effect on the population growth rate by a modification of the parameter.

5.1 Output population models

Lesser black-backed gull

Table 5.1 Summary lesser black-backed gull population level effects; Casualties represent the mean number of casualties across time periods, Abundance represents the maximum number of birds across time periods used as population size, Mortality is the mortality probability due to collisions. The median, 5% and 95% percentiles of the population growth rates (lambda) are also reported. P causality represents the probability that a violation of the X threshold results from an OWF induced impact. The last column shows whether P causality violates the ALI threshold.

Scenario	Casualties	Abundance	Mortality	Lambda median	5%	95%	P causality X = 30%	ALI 0.5
null	NA	NA	0	0.983	0.938	1.023	0	FALSE
Basic_2030	17	20553	0.005	0.978	0.933	1.019	0.166	FALSE
Rekenvariant_III	26	20553	0.007	0.975	0.93	1.016	0.24	FALSE
Rekenvariant_II	25	20553	0.007	0.976	0.931	1.017	0.223	FALSE
Rekenvariant_I	24	20553	0.007	0.976	0.931	1.017	0.22	FALSE
International	74	75351	0.006	0.977	0.932	1.018	0.2	FALSE

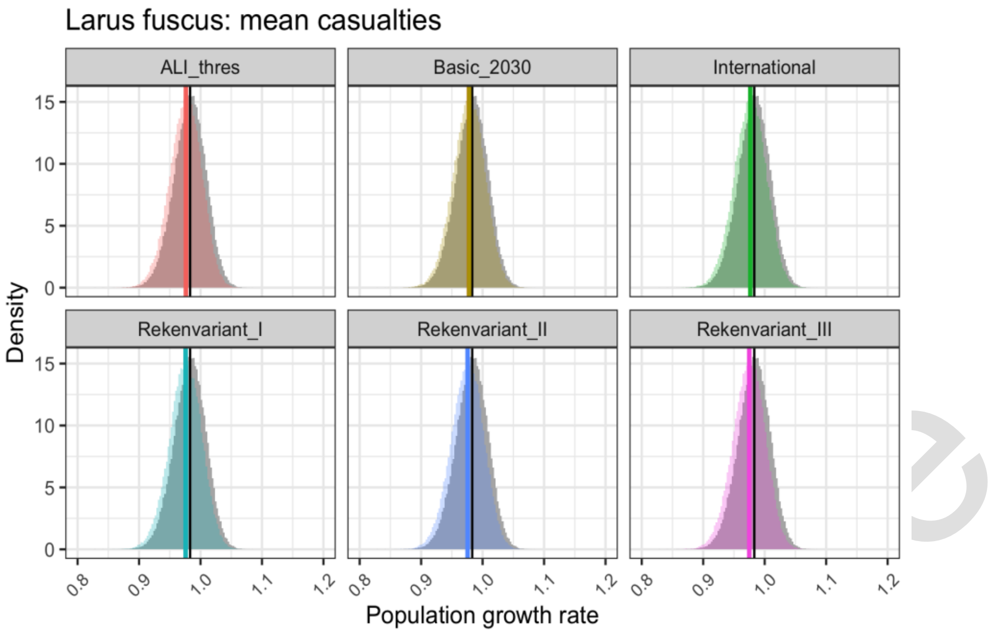

Figure 5.1 *Population growth rates per scenario for the lesser black-backed gull (*Larus fuscus*). Within each panel the distribution of the unimpacted population growth rate (grey bars) is compared with the distribution of the impacted population growth rate (coloured bars). Vertical lines indicate median population growth rates for unimpacted (black) and impacted (coloured) populations and the ALI threshold population growth rate (red).*

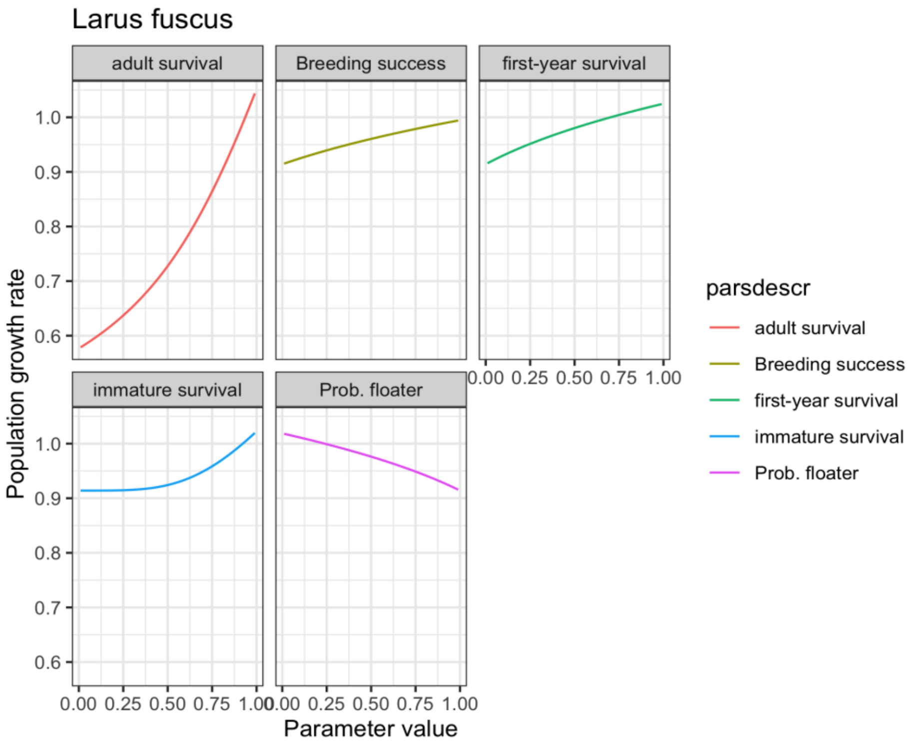

Figure 5.2 *Results of the sensitivity analysis for lesser black-backed gull (*Larus fuscus*). A steeper trend indicates a stronger effect on the population growth rate by a modification of the parameter.*

Herring gull

Table 5.2 *Summary herring gull population level effects; Casualties represent the mean number of casualties across time periods, Abundance represents the maximum number of birds across time periods used as population size, Mortality is the mortality probability due to collisions. The median, 5%and 95% percentiles of the population growth rates (lambda) are also reported. P causality represents the probability that a violation of the X threshold results from an OWF induced impact. The last column shows whether P causality violates the ALI threshold.*

Scenario	Casualties	Abundance	Mortality	Lambda median	5%	95%	P causality X = 15%	ALI 0.1
null	NA	NA	0	0.951	0.896	1	0	FALSE
Basic_2030	30	21139	0.008	0.942	0.887	0.992	0.203	TRUE
Rekenvariant_III	40	21139	0.011	0.939	0.884	0.989	0.246	TRUE
Rekenvariant_II	38	21139	0.011	0.939	0.885	0.99	0.238	TRUE
Rekenvariant_I	37	21139	0.01	0.94	0.885	0.99	0.232	TRUE
International	110	124965	0.005	0.945	0.891	0.994	0.134	TRUE

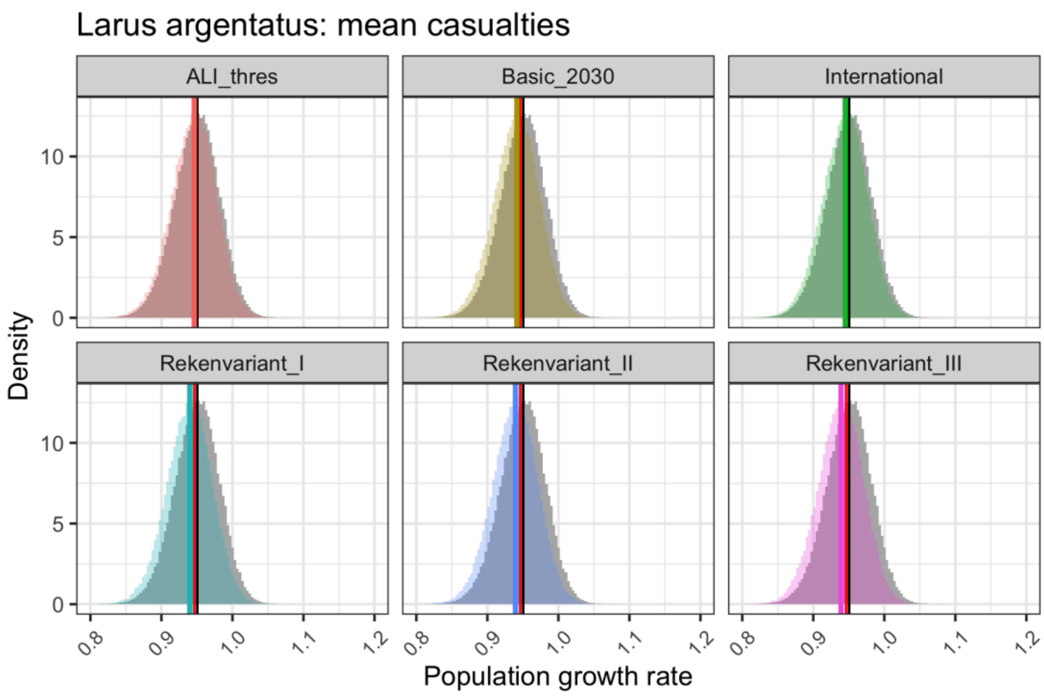

Figure 5.3 *Population growth rates per scenario for herring gull (Larus argentatus). Within each panel the distribution of the unimpacted population growth rate (grey bars) is compared with the distribution of the impacted population growth rate (coloured bars). Vertical lines indicate median population growth rates for unimpacted (black) and impacted (coloured) populations and the ALI threshold population growth rate (red).*

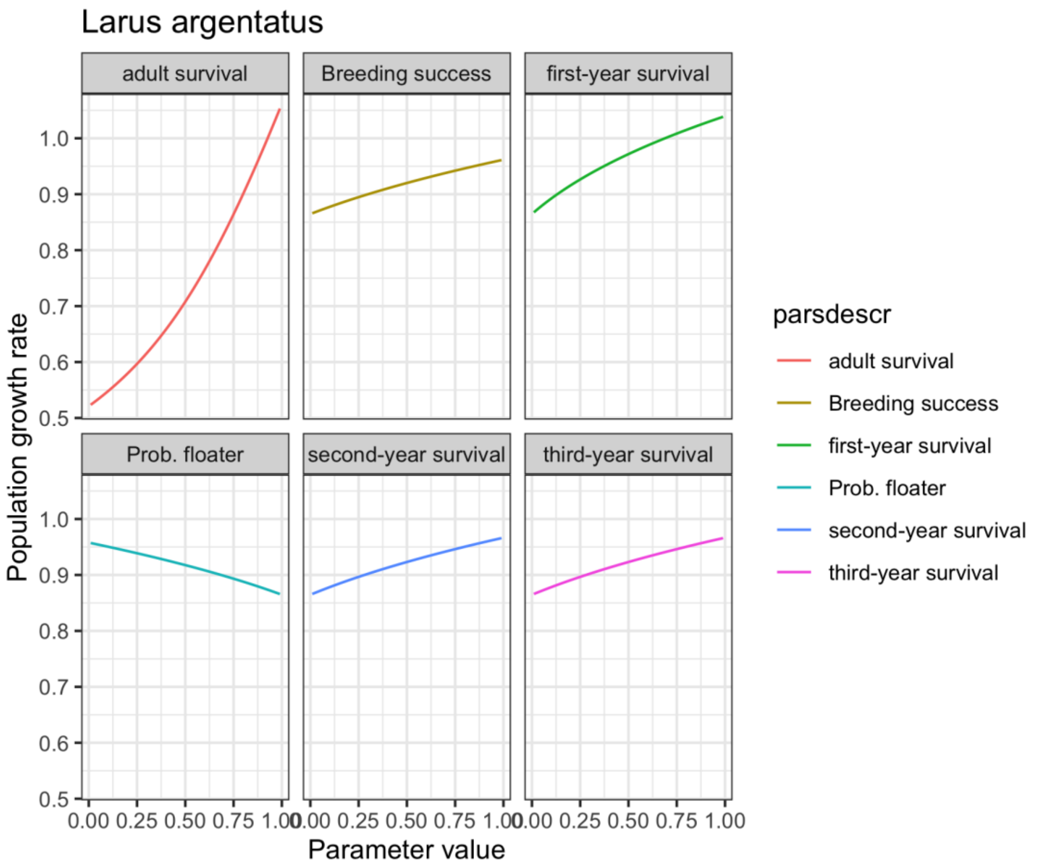

Figure 5.4 *Results of the sensitivity analysis for herring gull (Larus argentatus). A steeper trend indicates a stronger effect on the population growth rate by a modification of the parameter.*

Little gull

Table 5.3 *Summary little gull population level effects; Casualties represent the mean number of casualties across time periods, Abundance represents the maximum number of birds across time periods used as population size, Mortality is the mortality probability due to collisions. The median, 5%and 95% percentiles of the population growth rates (lambda) are also reported. P causality represents the probability that a violation of the X threshold results from an impact. The last column shows whether P causality violates the ALI threshold.*

Scenario	Casualties	Abundance	Mortality	Lambda median	5%	95%	P causality X = 30%	ALI 0.5
null	NA	NA	0	1.009	0.934	1.078	0	FALSE
Basic_2030	16	57833	0.002	1.007	0.932	1.076	0.035	FALSE
Rekenvariant_III	20	57833	0.002	1.007	0.932	1.076	0.043	FALSE
Rekenvariant_II	19	57833	0.002	1.006	0.932	1.076	0.047	FALSE
Rekenvariant_I	19	57833	0.002	1.007	0.932	1.076	0.047	FALSE
International	24	55817	0.003	1.006	0.932	1.075	0.048	FALSE

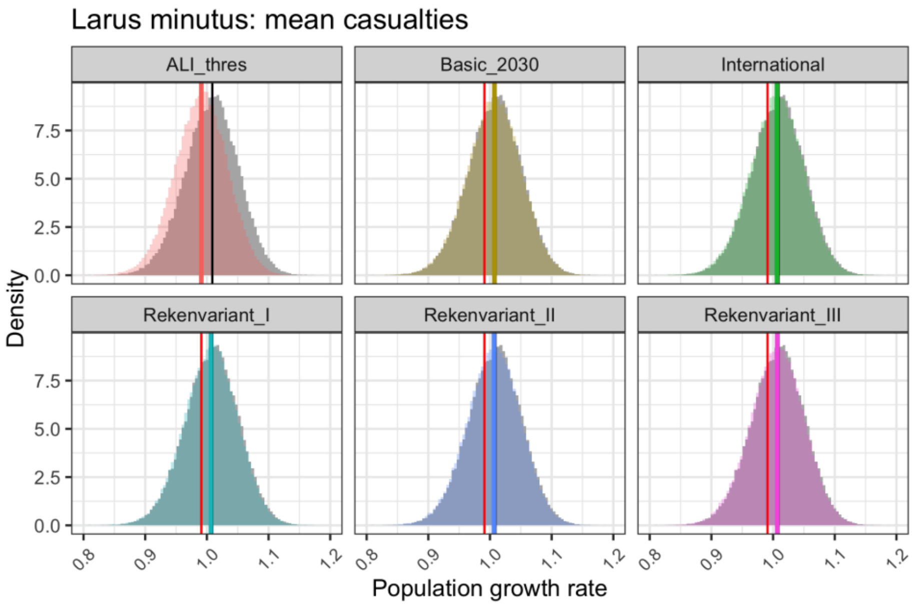

Figure 5.5 *Population growth rates per scenario for little gull (Larus minutus). Within each panel the distribution of the unimpacted population growth rate (grey bars) is compared with the distribution of the impacted population growth rate (coloured bars). Vertical lines indicate median population growth rates for unimpacted (black) and impacted (coloured) populations and the ALI threshold population growth rate (red).*

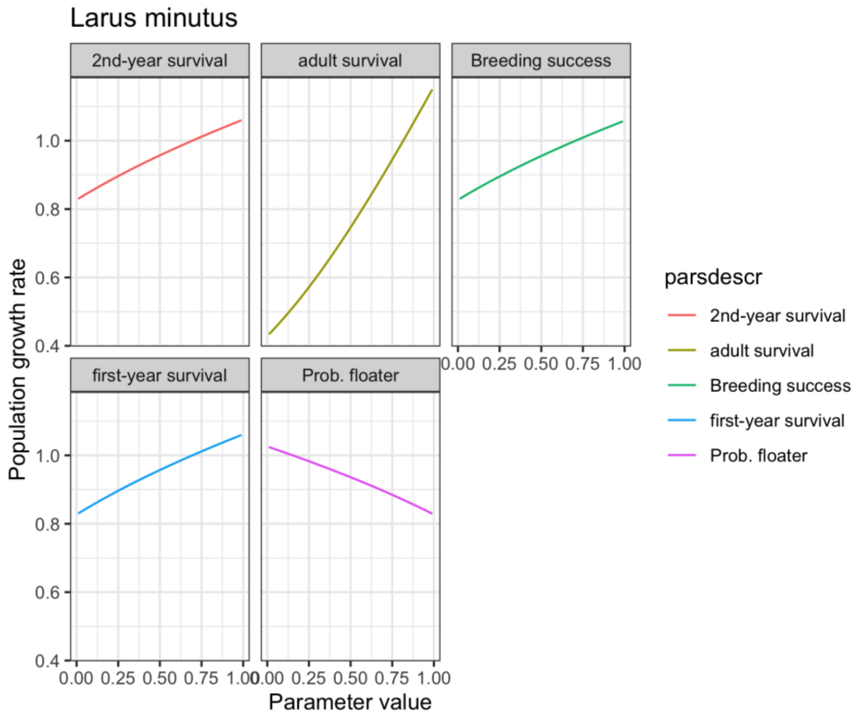

Figure 5.6 *Results of the sensitivity analysis for the little gull (Larus minutus). A steeper trend indicates a stronger effect on the population growth rate by a modification of the parameter.*

Great black-backed gull

Table 5.4 *Summary great black-backed gull population level effects; Casualties represent the mean number of casualties across time periods, Abundance represents the maximum number of birds across time periods used as population size, Mortality is the mortality probability due to collisions. The median, 5%and 95% percentiles of the population growth rates (lambda) are also reported. P causality represents the probability that a violation of the X threshold results from an OWF induced impact. The last column shows whether P causality violates the ALI threshold.*

Scenario	Casualties	Abundance	Mortality	Lambda median	5%	95%	P causality X = 30%	ALI 0.5
null	NA	NA	0	0.948	0.887	1.005	0	FALSE
Basic_2030	57	16264	0.021	0.93	0.871	0.984	0.35	FALSE
Rekenvariant_III	112	16264	0.04	0.913	0.857	0.965	0.503	TRUE
Rekenvariant_II	97	16264	0.035	0.917	0.861	0.97	0.471	FALSE
Rekenvariant_I	92	16264	0.033	0.919	0.862	0.972	0.461	FALSE
International	363	92417	0.023	0.928	0.869	0.982	0.374	FALSE

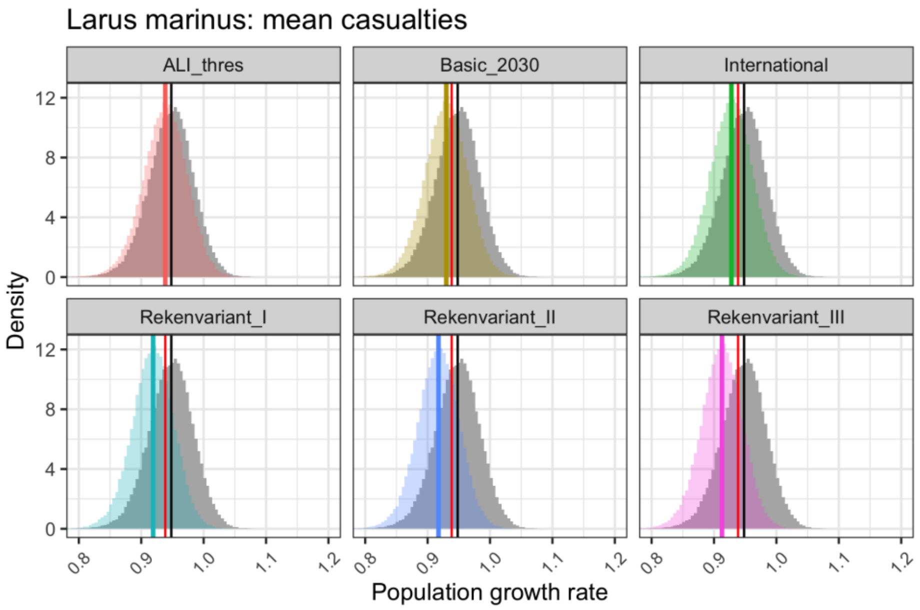

Figure 5.7 *Population growth rates per scenario for great black-backed gull (Larus marinus). Within each panel the distribution of the unimpacted population growth rate (grey bars) is compared with the distribution of the impacted population growth rate (coloured bars). Vertical lines indicate median population growth rates for unimpacted (black) and impacted (coloured) populations and the ALI threshold population growth rate (red).*

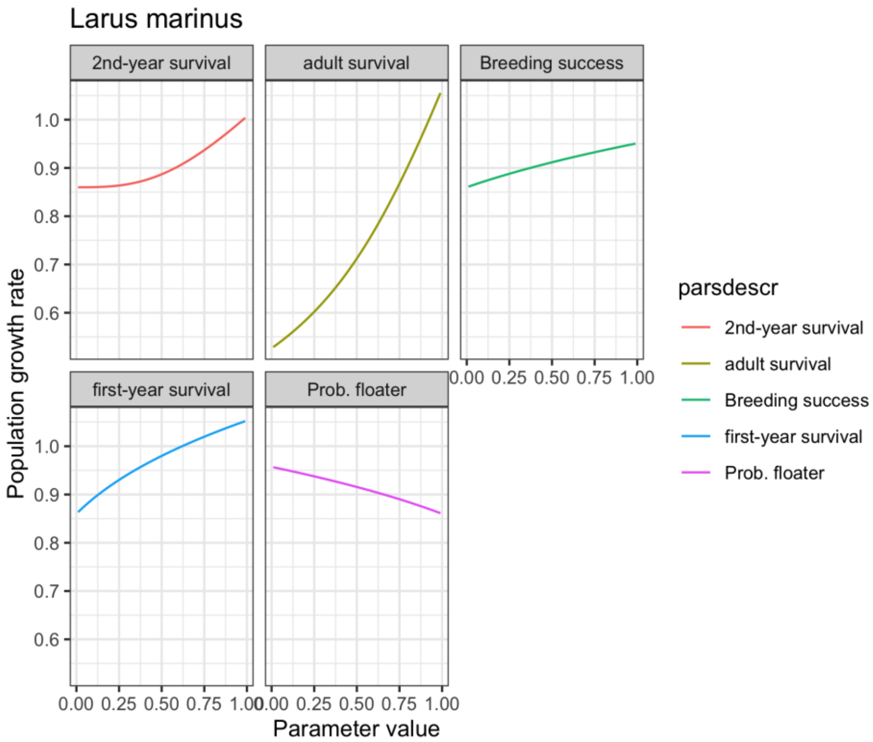

Figure 5.8 *Results of the sensitivity analysis for the great black-backed gull (Larus marinus). A steeper trend indicates a stronger effect on the population growth rate by a modification of the parameter.*

Black-legged kittiwake

Table 5.5 *Summary black-legged kittiwake population level effects; Casualties represent the mean number of casualties across time periods, Abundance represents the maximum number of birds across time periods used as population size, Mortality is the mortality probability due to collisions. The median, 5%and 95% percentiles of the population growth rates (lambda) are also reported. P causality represents the probability that a violation of the X threshold results from an OWF induced impact. The last column shows whether P causality violates the ALI threshold.*

Scenario	Casualties	Abundance	Mortality	Lambda median	5%	95%	P causality X = 15%	ALI 0.1
null	NA	NA	0	0.951	0.866	1.018	0	FALSE
Basic_2030	39	78922	0.003	0.948	0.862	1.016	0.052	FALSE
Rekenvariant_III	71	78922	0.005	0.945	0.859	1.013	0.096	TRUE
Rekenvariant_II	64	78922	0.005	0.946	0.86	1.014	0.085	FALSE
Rekenvariant_I	61	78922	0.005	0.946	0.86	1.014	0.08	FALSE
International	212	444164	0.003	0.948	0.862	1.016	0.048	FALSE

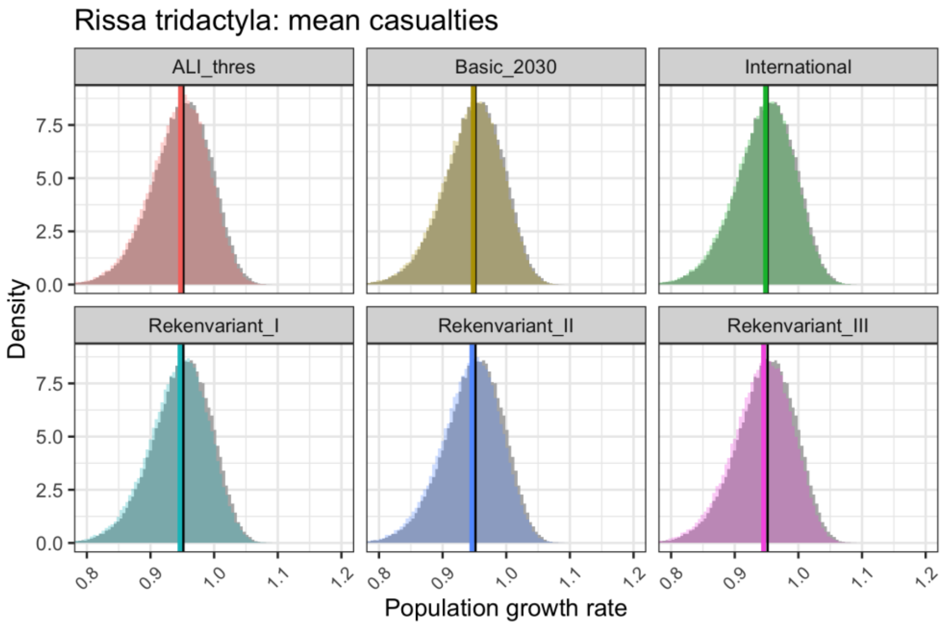

Figure 5.9 *Population growth rates per scenario for black-legged kittiwake (Rissa tridactyla). Within each panel the distribution of the unimpacted population growth rate (grey bars) is compared with the distribution of the impacted population growth rate (coloured bars). Vertical lines indicate median population growth rates for unimpacted (black) and impacted (coloured) populations and the ALI threshold population growth rate (red).*

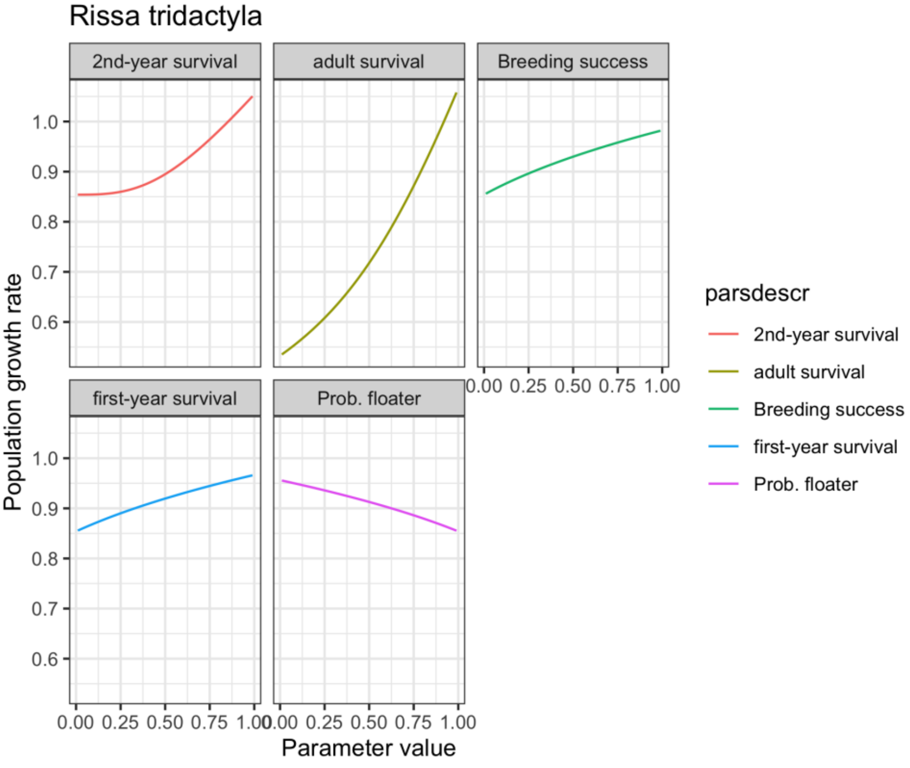

Figure 5.10 *Results of the sensitivity analysis for black-legged kittiwake (Rissa tridactyla). A steeper trend indicates a stronger effect on the population growth rate by a modification of the parameter.*

Northern gannet

Table 5.6 *Summary northern gannet population level effects; Casualties represent the mean number of casualties across time periods, Abundance represents the maximum number of birds across time periods used as population size, Mortality is the mortality probability due to collisions and habitat loss combined. The median, 5%and 95% percentiles of the population growth rates (lambda) are also reported. P causality represents the probability that a violation of the X threshold results from an OWF induced impact. The last column shows whether P causality violates the ALI threshold.*

Scenario	Casualties	Abundance	Mortality	Lambda median	5%	95%	P causality X = 30%	ALI 0.5
null	NA	NA	0	1.009	0.966	1.045	0	FALSE
Basic_2030	204	31859	0.038	0.968	0.924	1.005	0.595	TRUE
Rekenvariant_III	332	31859	0.061	0.943	0.898	0.981	0.621	TRUE
Rekenvariant_II	305	31859	0.056	0.948	0.904	0.986	0.62	TRUE
Rekenvariant_I	291	31859	0.054	0.951	0.906	0.988	0.619	TRUE
International	1209	162868	0.044	0.961	0.917	0.999	0.608	TRUE

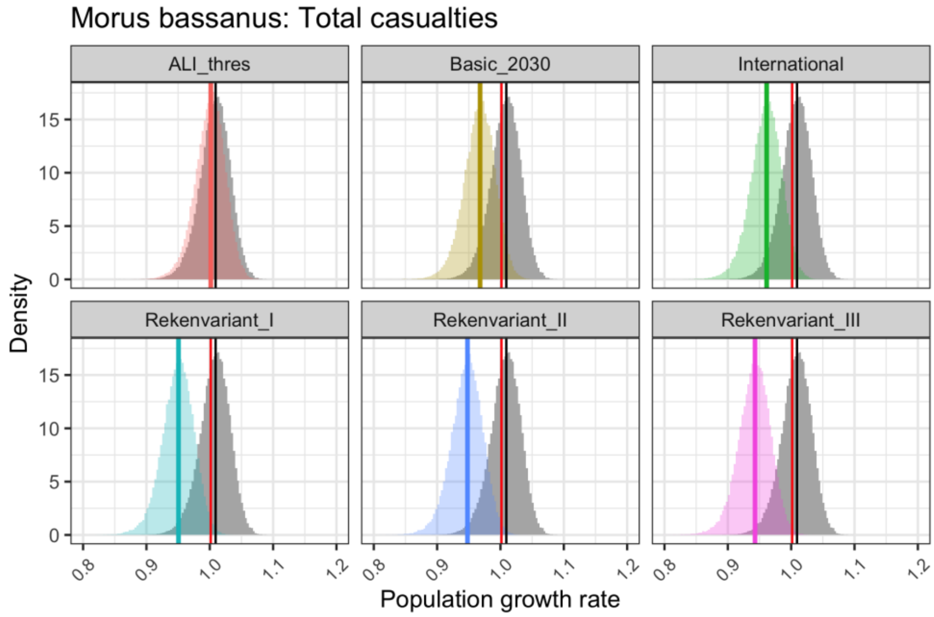

Figure 5.11 *Population growth rates per scenario for the northern gannet (Morus bassanus). Within each panel the distribution of the unimpacted population growth rate (grey bars) is compared with the distribution of the impacted population growth rate (coloured bars). Vertical lines indicate median population growth rates for unimpacted (black) and impacted (coloured) populations and the ALI threshold population growth rate (red).*

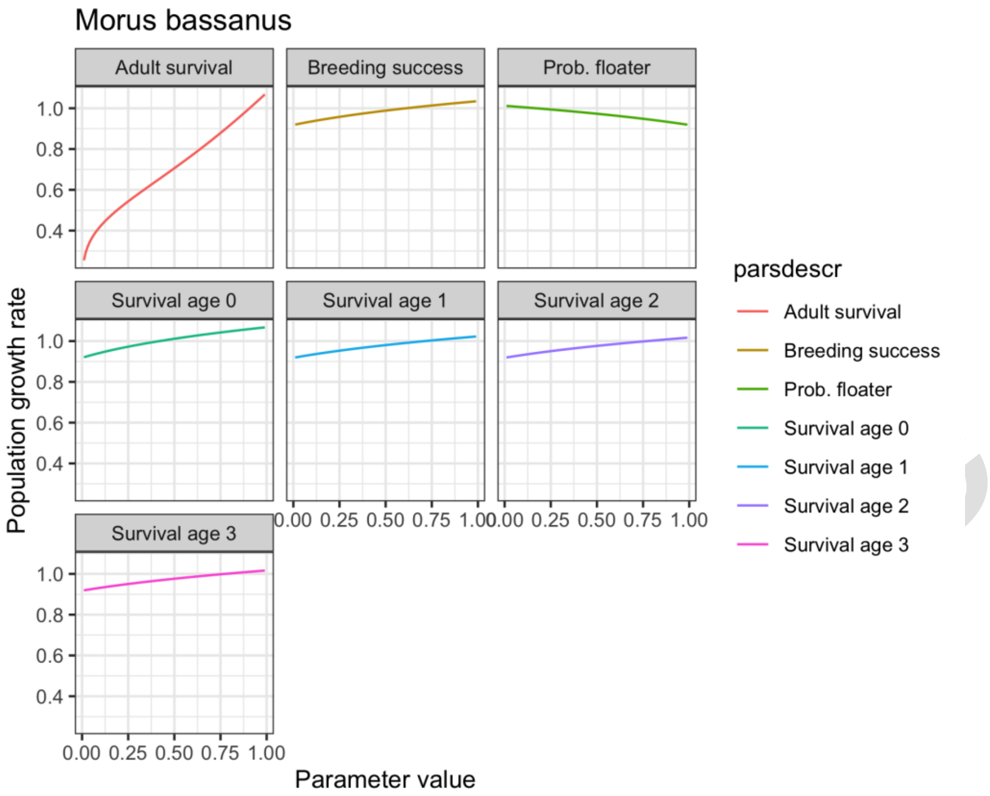

Figure 5.12 *Results of the sensitivity analysis for the northern gannet (Morus bassanus). A steeper trend indicates a stronger effect on the population growth rate by a modification of the parameter.*

Arctic skua

Table 5.7 *Summary arctic skua population level effects; Casualties represent the mean number of casualties across time periods, Abundance represents the maximum number of birds across time periods used as population size, Mortality is the mortality probability due to collisions. The median, 5%and 95% percentiles of the population growth rates (lambda) are also reported. P causality represents the probability that a violation of the X threshold results from an OWF induced impact. The last column shows whether P causality violates the ALI threshold.*

Scenario	Casualties	Abundance	Mortality	Lambda median	5%	95%	P causality X = 15%	ALI 0.1
null	NA	NA	0	0.961	0.873	1.018	0	FALSE
Basic_2030	1	131	0.001	0.96	0.873	1.017	0.012	FALSE
Rekenvariant_III	1	131	0.001	0.96	0.873	1.017	0.005	FALSE
Rekenvariant_II	1	131	0.001	0.96	0.873	1.017	0.007	FALSE
Rekenvariant_I	1	131	0.001	0.96	0.872	1.017	0.012	FALSE
International	1	3186	0.001	0.961	0.872	1.017	0.004	FALSE

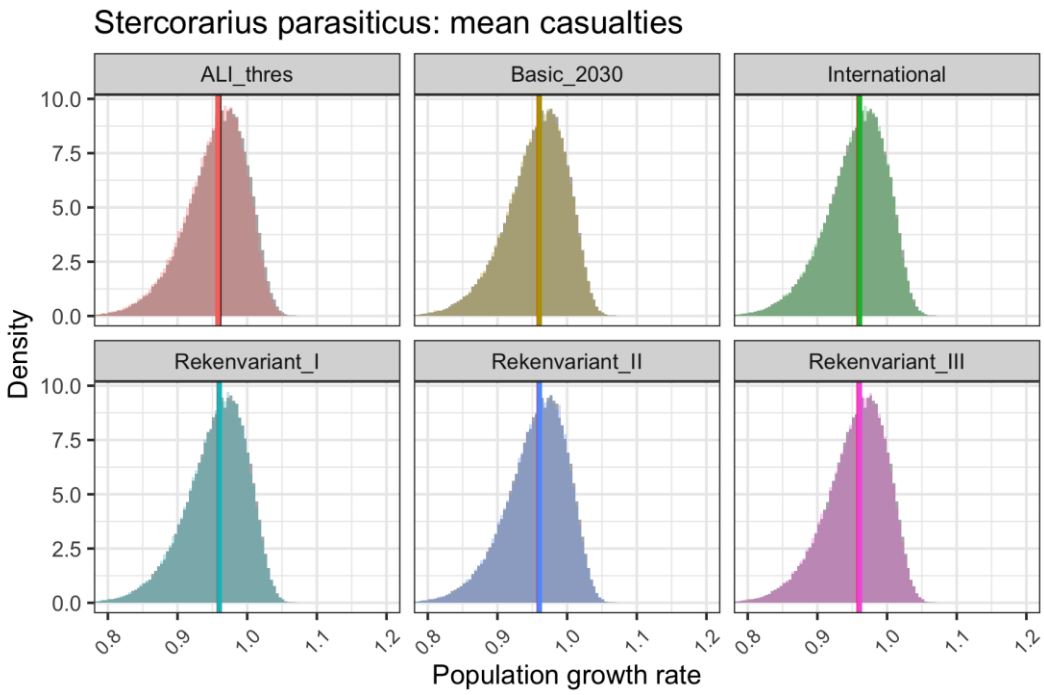

Figure 5.13 *Population growth rates per scenario for the arctic skua* (Stercorarius parasiticus). *Within each panel the distribution of the unimpacted population growth rate (grey bars) is compared with the distribution of the impacted population growth rate (coloured bars). Vertical lines indicate median population growth rates for unimpacted (black) and impacted (coloured) populations and the ALI threshold population growth rate (red).*

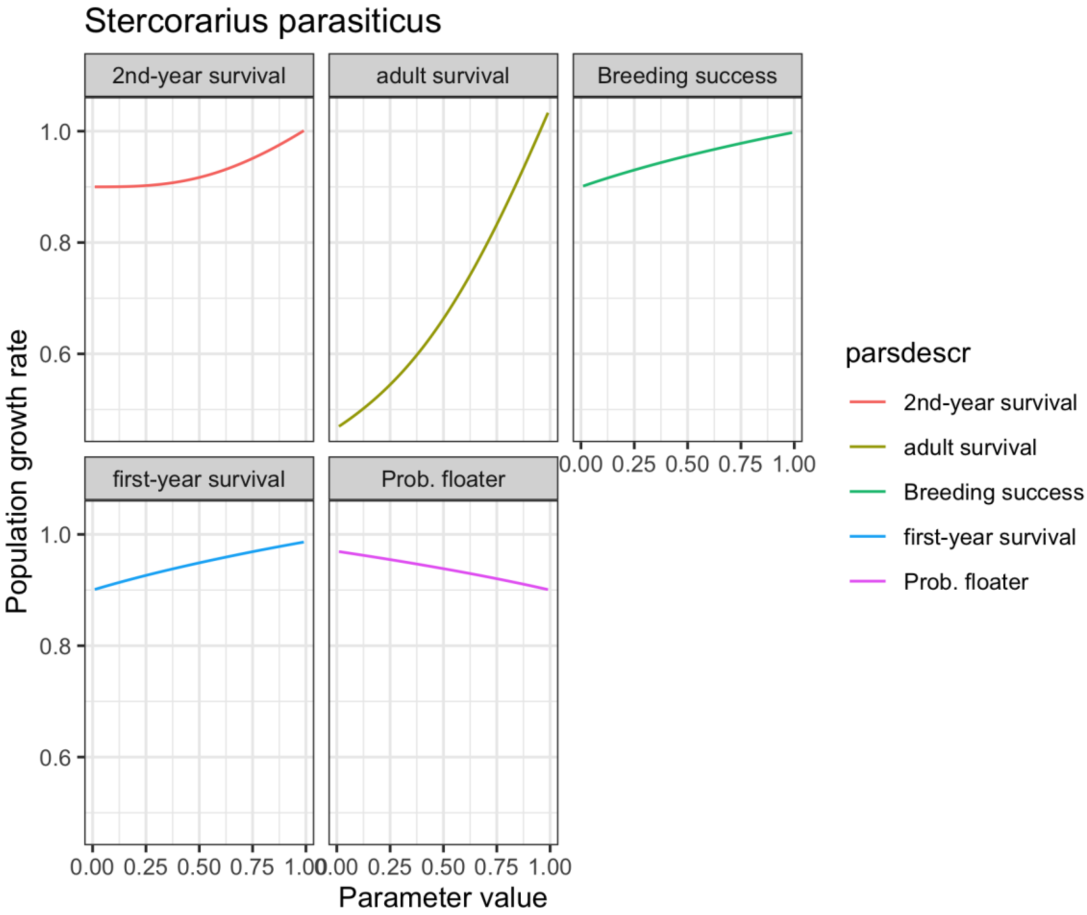

Figure 5.14 *Results of the sensitivity analysis for the arctic skua* (Stercorarius parasiticus). *A steeper trend indicates a stronger effect on the population growth rate by a modification of the parameter.*

Great skua

Table 5.8 *Summary great skua population level effects; Casualties represent the mean number of casualties across time periods, Abundance represents the maximum number of birds across time periods used as population size, Mortality is the mortality probability due to collisions. The median, 5%and 95% percentiles of the population growth rates (lambda) are also reported. P causality represents the probability that a violation of the X threshold results from an OWF induced impact. The last column shows whether P causality violates the ALI threshold.*

Scenario	Casualties	Abundance	Mortality	Lambda median	5%	95%	P causality X = 30%	ALI 0.5
null	NA	NA	0	0.956	0.856	1.029	0	FALSE
Basic_2030	1	1365	0.001	0.954	0.855	1.027	0.025	FALSE
Rekenvariant_III	1	1365	0.004	0.95	0.852	1.024	0.085	FALSE
Rekenvariant_II	1	1365	0.004	0.951	0.852	1.025	0.073	FALSE
Rekenvariant_I	1	1365	0.003	0.951	0.852	1.025	0.07	FALSE
International	5	12103	0.002	0.953	0.853	1.026	0.052	FALSE

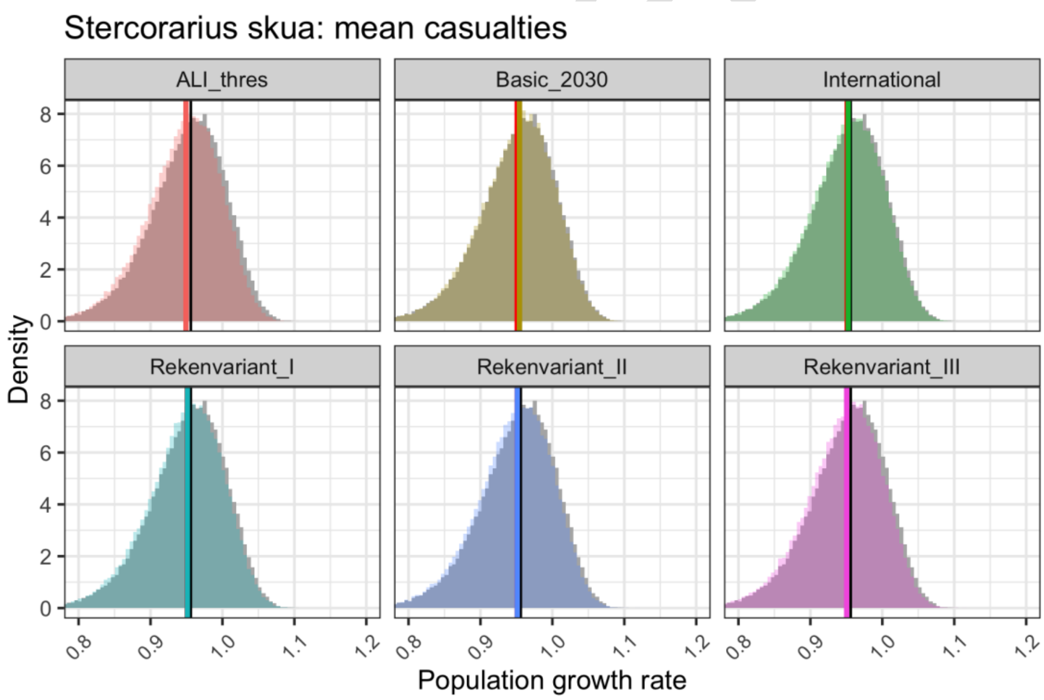

Figure 5.15 *Population growth rates per scenario for the great skua* (Stercorarius skua). *Within each panel the distribution of the unimpacted population growth rate (grey bars) is compared with the distribution of the impacted population growth rate (coloured bars). Vertical lines indicate median population growth rates for unimpacted (black) and impacted (coloured) populations and the ALI threshold population growth rate (red).*

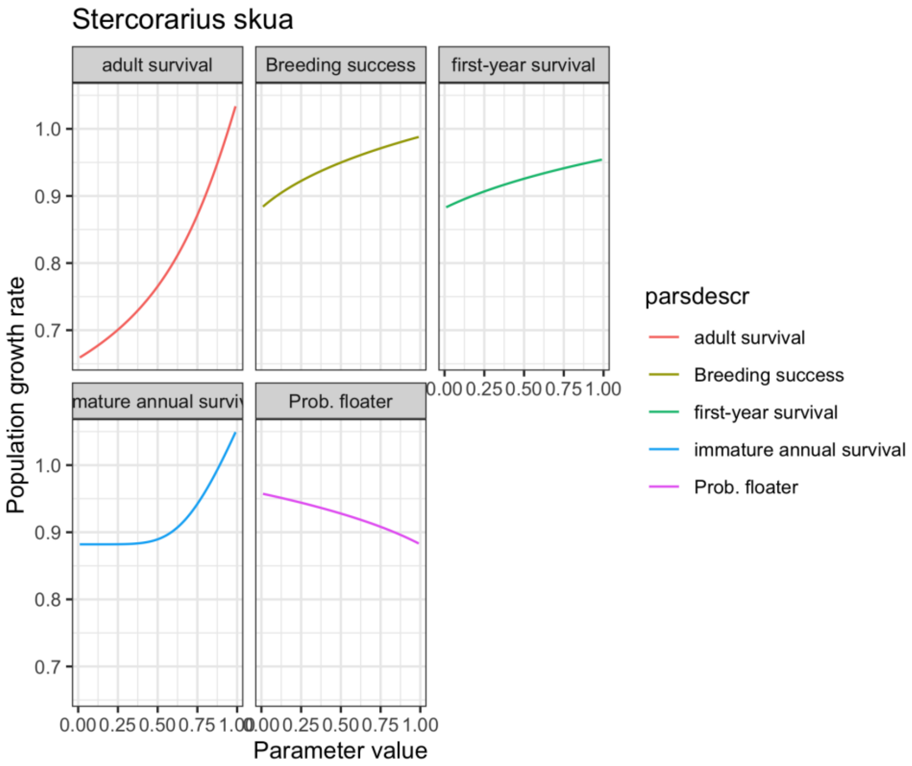

Figure 5.14 *Results of the sensitivity analysis for the great skua* (Stercorarius skua). *A steeper trend indicates a stronger effect on the population growth rate by a modification of the parameter.*

Common tern

Table 5.9 *Summary common tern population level effects; Casualties represent the mean number of casualties across time periods, Abundance represents the maximum number of birds across time periods used as population size, Mortality is the mortality probability due to collisions. The median, 5%and 95% percentiles of the population growth rates (lambda) are also reported. P causality represents the probability that a violation of the X threshold results from an OWF induced impact. The last column shows whether P causality violates the ALI threshold.*

Scenario	Casualties	Abundance	Mortality	Lambda median	5%	95%	P causality X = 30%	ALI 0.5
null	NA	NA	0	0.997	0.905	1.058	0	FALSE
Basic_2030	8	59093	0.001	0.996	0.904	1.057	0.015	FALSE
Rekenvariant_III	10	59093	0.001	0.996	0.904	1.057	0.025	FALSE
Rekenvariant_II	10	59093	0.001	0.996	0.904	1.057	0.016	FALSE
Rekenvariant_I	10	59093	0.001	0.996	0.903	1.057	0.018	FALSE
International	17	74948	0.001	0.996	0.904	1.056	0.027	FALSE

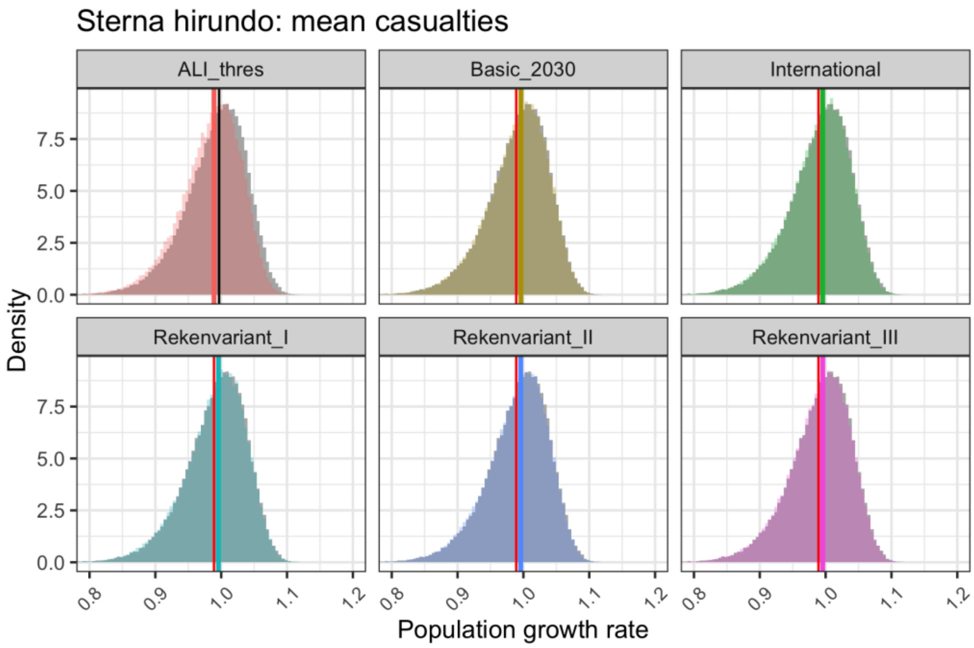

Figure 5.16 *Population growth rates per scenario for the common tern* (Sterna hirundo). *Within each panel the distribution of the unimpacted population growth rate (grey bars) is compared with the distribution of the impacted population growth rate (coloured bars). Vertical lines indicate median population growth rates for unimpacted (black) and impacted (coloured) populations and the ALI threshold population growth rate (red).*

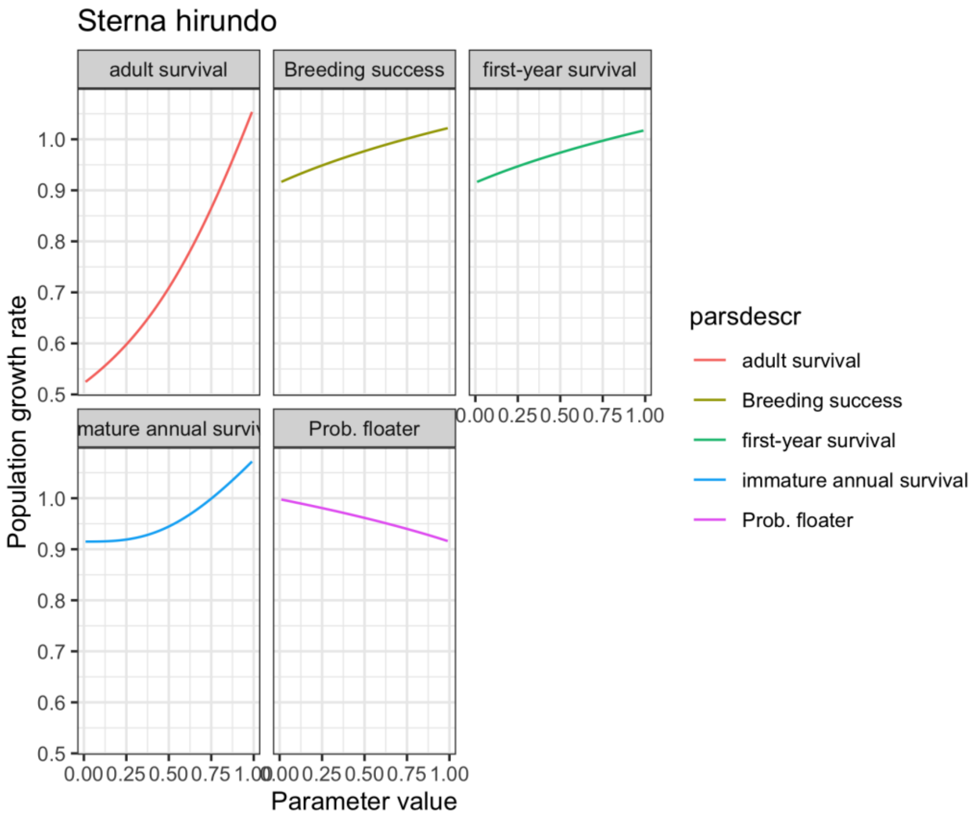

Figure 5.16 *Results of the sensitivity analysis for the common tern* (Sterna hirundo). *A steeper trend indicates a stronger effect on the population growth rate by a modification of the parameter.*

Sandwich tern

Table 5.10 *Summary Sandwich tern population level effects; Casualties represent the mean number of casualties across time periods, Abundance represents the maximum number of birds across time periods used as population size, Mortality is the mortality probability due to collisions. The median, 5%and 95% percentiles of the population growth rates (lambda) are also reported. P causality represents the probability that a violation of the X threshold results from an OWF induced impact. The last column shows whether P causality violates the ALI threshold.*

Scenario	Casualties	Abundance	Mortality	Lambda median	5%	95%	P causality X = 30%	ALI 0.5
null	NA	NA	0	1.043	0.801	1.118	0	FALSE
Basic_2030	6	22603	0.001	1.042	0.802	1.117	0.019	FALSE
Rekenvariant_III	7	22603	0.002	1.043	0.801	1.117	0.014	FALSE
Rekenvariant_II	7	22603	0.002	1.042	0.804	1.117	0.018	FALSE
Rekenvariant_I	7	22603	0.002	1.042	0.801	1.118	0.018	FALSE
International	11	25882	0.002	1.042	0.801	1.117	0.031	FALSE

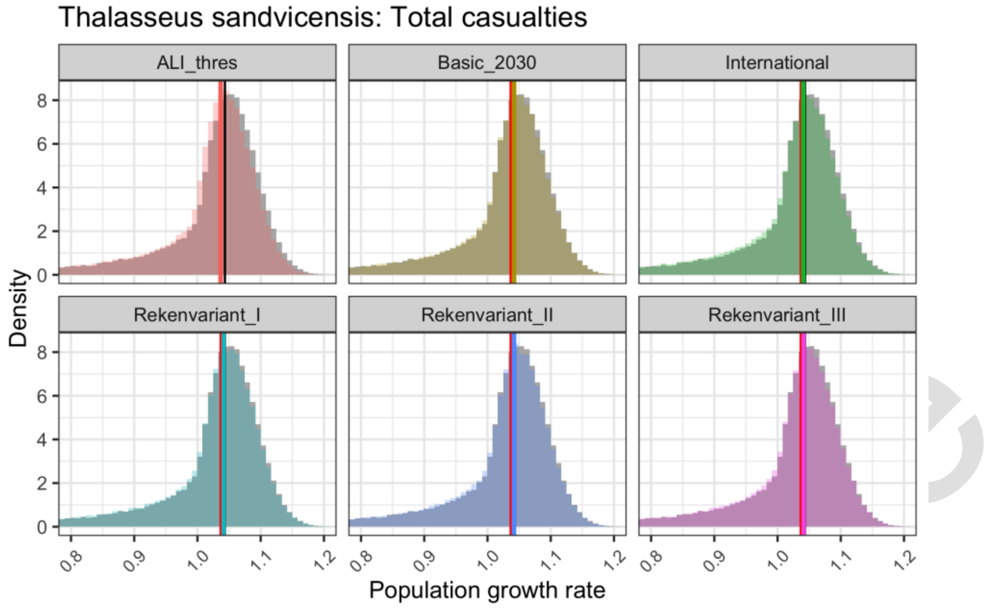

Figure 5.17 *Population growth rates per scenario for the Sandwich tern* (Thalasseus sandvicensis). *Within each panel the distribution of the unimpacted population growth rate (grey bars) is compared with the distribution of the impacted population growth rate (coloured bars). Vertical lines indicate median population growth rates for unimpacted (black) and impacted (coloured) populations and the ALI threshold population growth rate (red).*

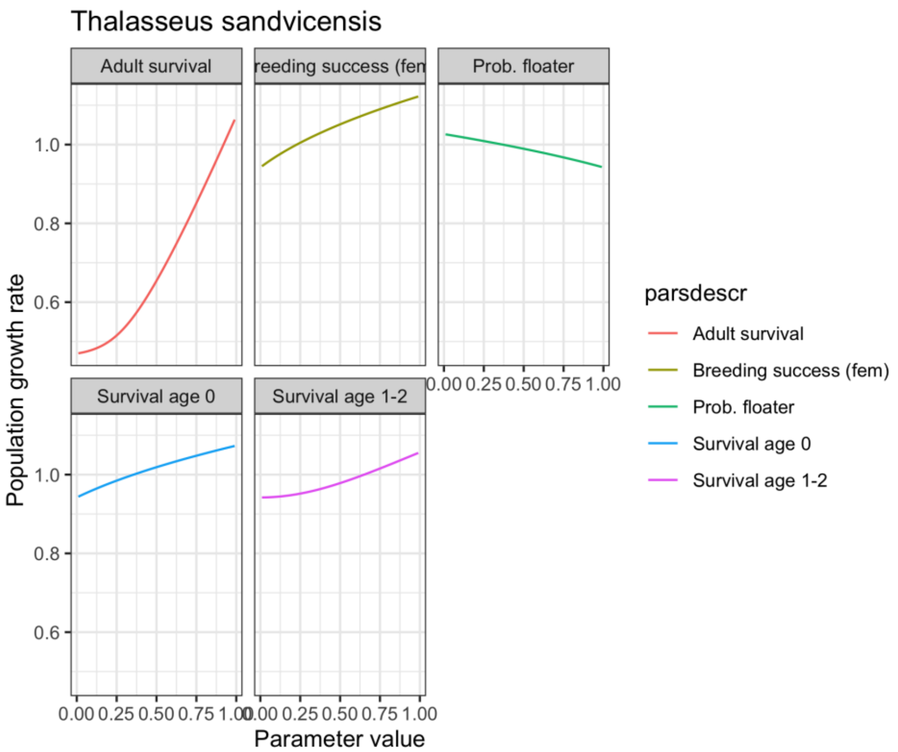

Figure 18 *Results of the sensitivity analysis for the Bewick's swan (Cygnus columbianus). A steeper trend indicates a stronger effect on the population growth rate by a modification of the parameter.*

Bewick's swan

Table 5.11 *Summary Bewick's swan population level effects; Casualties represent the mean number of casualties across time periods, Abundance represents the maximum number of birds across time periods used as population size, Mortality is the mortality probability due to collisions. The median, 5%and 95% percentiles of the population growth rates (lambda) are also reported. P causality represents the probability that a violation of the X threshold results from an OWF induced impact. The last column shows whether P causality violates the ALI threshold.*

Scenario	Casualties	Abundance	Mortality	Lambda median	5%	95%	P causality X = 15%	ALI 0.1
null	NA	NA	0	0.993	0.889	1.084	0	FALSE
Basic_2030	3	17450	0	0.994	0.89	1.084	0	FALSE
Rekenvariant_III	5	17450	0	0.994	0.89	1.084	0	FALSE
Rekenvariant_II	5	17450	0	0.993	0.889	1.084	0.006	FALSE
Rekenvariant_I	4	17450	0	0.993	0.889	1.084	0.007	FALSE
International	10	17450	0.001	0.993	0.888	1.084	0.008	FALSE

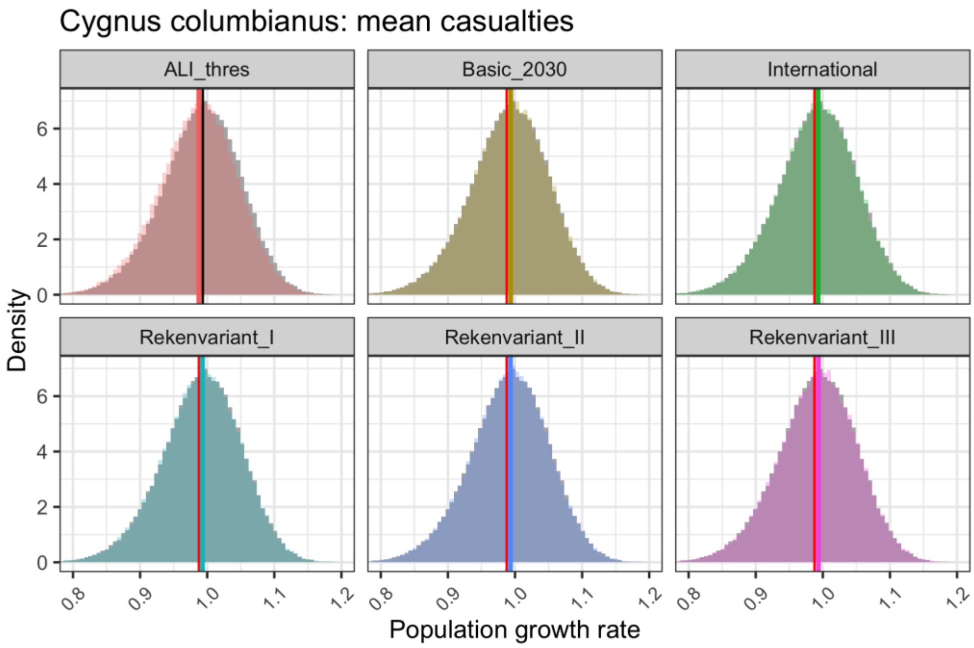

Figure 5.19 *Population growth rates per scenario for the Bewick's swan* (Cygnus columbianus bewickii). *Within each panel the distribution of the unimpacted population growth rate (grey bars) is compared with the distribution of the impacted population growth rate (coloured bars). Vertical lines indicate median population growth rates for unimpacted (black) and impacted (coloured) populations and the ALI threshold population growth rate (red).*

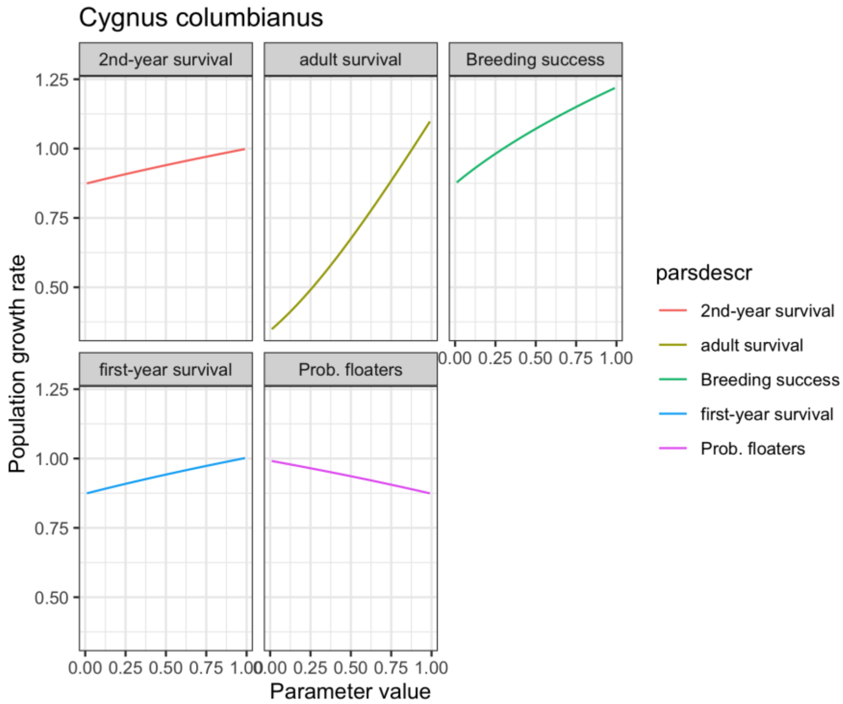

Figure 5.20 *Results of the sensitivity analysis for the Bewick's swan (Cygnus columbianus). A steeper trend indicates a stronger effect on the population growth rate by a modification of the parameter.*

Brent goose

Table 5.12 *Summary brent goose population level effects; Casualties represent the mean number of casualties across time periods, Abundance represents the maximum number of birds across time periods used as population size, Mortality is the mortality probability due to collisions. The median, 5%and 95% percentiles of the population growth rates (lambda) are also reported. P causality represents the probability that a violation of the X threshold results from an OWF induced impact. The last column shows whether P causality violates the ALI threshold.*

Scenario	Casualties	Abundance	Mortality	Lambda median	5%	95%	P causality X = 30%	ALI 0.5
null	NA	NA	0	0.996	0.935	1.052	0	FALSE
Basic_2030	23	247286	0	0.996	0.935	1.051	0.006	FALSE
Rekenvariant_III	46	247286	0	0.996	0.935	1.052	0.004	FALSE
Rekenvariant_II	44	247286	0	0.996	0.935	1.052	0.001	FALSE
Rekenvariant_I	39	247286	0	0.997	0.935	1.052	0	FALSE
International	93	247286	0	0.996	0.935	1.052	0	FALSE

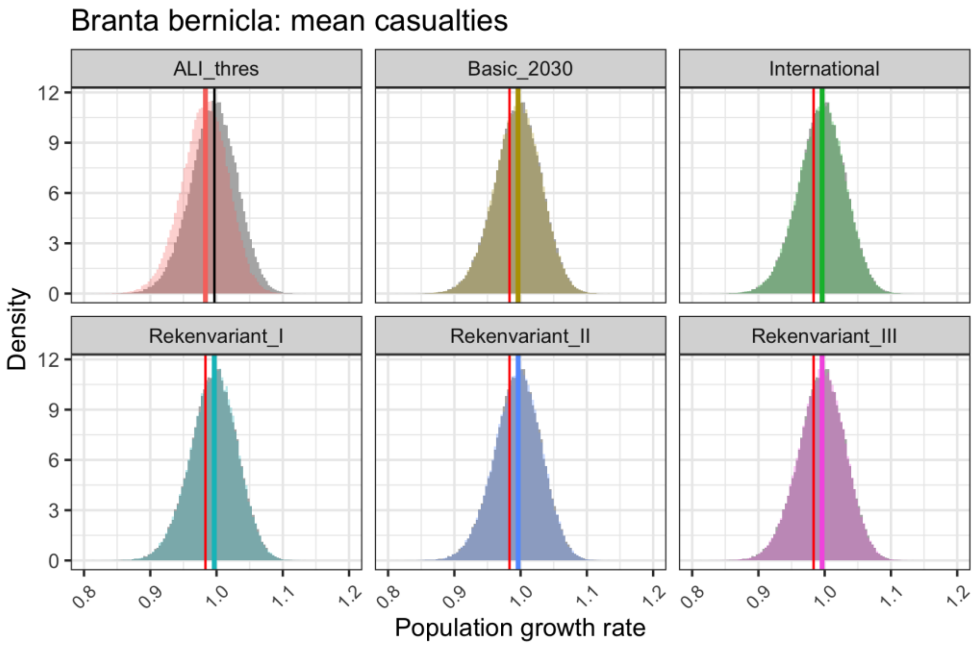

Figure 5.21 *Population growth rates per scenario for the brent goose (Branta bernicla). Within each panel the distribution of the unimpacted population growth rate (grey bars) is compared with the distribution of the impacted population growth rate (coloured bars). Vertical lines indicate median population growth rates for unimpacted (black) and impacted (coloured) populations and the ALI threshold population growth rate (red).*

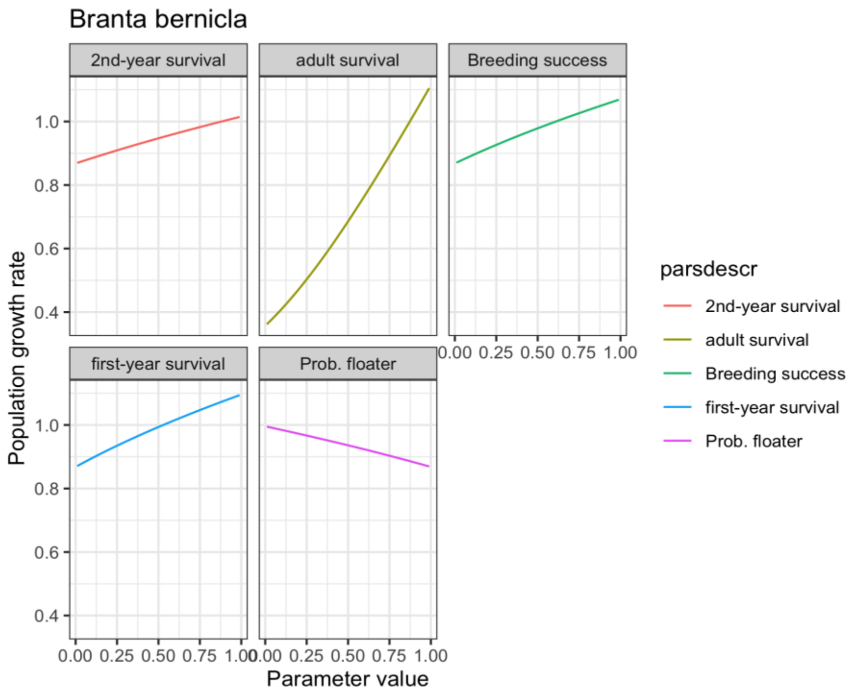

Figure 5.22 *Results of the sensitivity analysis for the brent goose (*Branta bernicla*). A steeper trend indicates a stronger effect on the population growth rate by a modification of the parameter.*

Common shelduck

Table 5.13 *Summary common shelduck population level effects; Casualties represent the mean number of casualties across time periods, Abundance represents the maximum number of birds across time periods used as population size, Mortality is the mortality probability due to collisions. The median, 5%and 95% percentiles of the population growth rates (lambda) are also reported. P causality represents the probability that a violation of the X threshold results from an OWF induced impact. The last column shows whether P causality violates the ALI threshold.*

Scenario	Casualties	Abundance	Mortality	Lambda median	5%	95%	P causality X = 30%	ALI 0.5
null	NA	NA	0	1.064	0.966	1.15	0	FALSE
Basic_2030	64	302047	0	1.064	0.965	1.15	0.005	FALSE
Rekenvariant_III	128	302047	0	1.063	0.965	1.149	0.013	FALSE
Rekenvariant_II	114	302047	0	1.064	0.966	1.149	0.012	FALSE
Rekenvariant_I	106	302047	0	1.064	0.965	1.149	0.011	FALSE
International	473	302047	0.002	1.063	0.964	1.148	0.033	FALSE

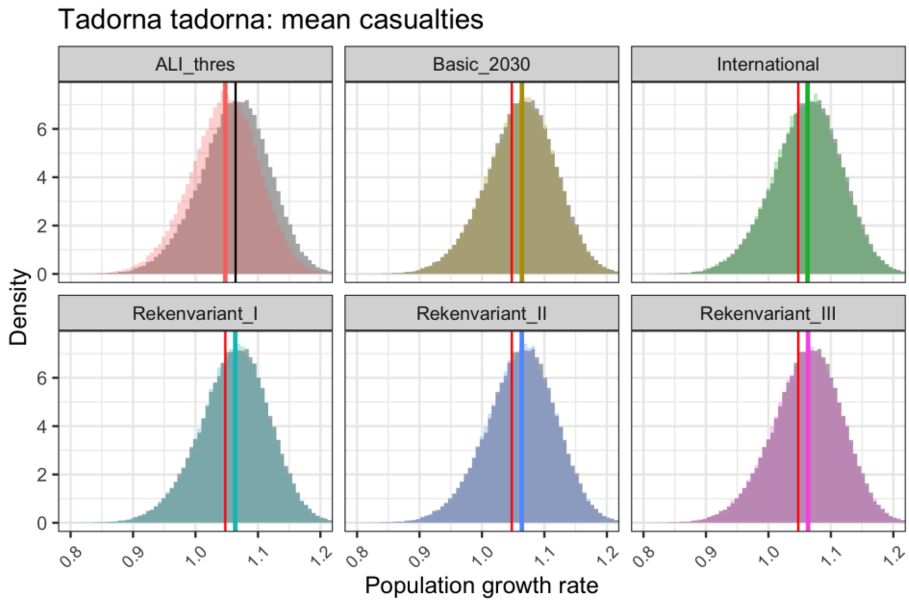

Figure 5.23 *Population growth rates per scenario for the common shelduck (Tadorna tadorna). Within each panel the distribution of the unimpacted population growth rate (grey bars) is compared with the distribution of the impacted population growth rate (coloured bars). Vertical lines indicate median population growth rates for unimpacted (black) and impacted (coloured) populations and the ALI threshold population growth rate (red).*

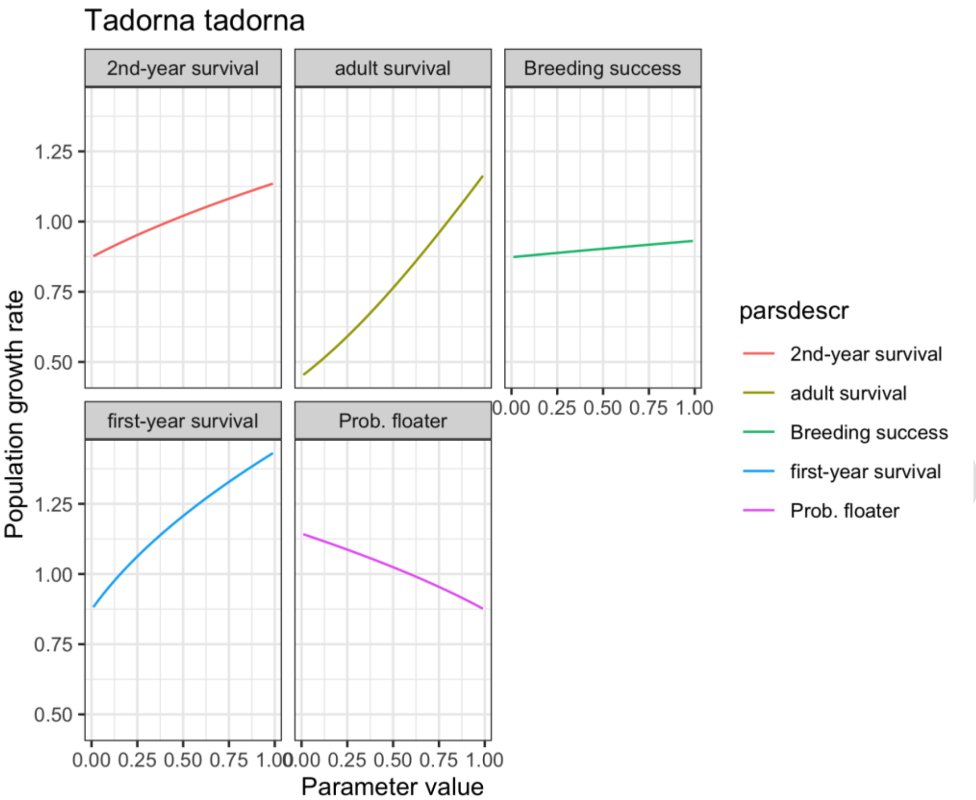

Figure 5.24 *Results of the sensitivity analysis for the common shelduck* (Tadorna tadorna). *A steeper trend indicates a stronger effect on the population growth rate by a modification of the parameter.*

Eurasian curlew

Table 5.14 *Summary Eurasian curlew population level effects; Casualties represent the mean number of casualties across time periods, Abundance represents the maximum number of birds across time periods used as population size, Mortality is the mortality probability due to collisions. The median, 5%and 95% percentiles of the population growth rates (lambda) are also reported. P causality represents the probability that a violation of the X threshold results from an OWF induced impact. The last column shows whether P causality violates the ALI threshold.*

Scenario	Casualties	Abundance	Mortality	Lambda median	5%	95%	P causality X = 15%	ALI 0.1
null	NA	NA	0	0.986	0.885	1.05	0	FALSE
Basic_2030	91	302273	0	0.986	0.886	1.049	0.003	FALSE
Rekenvariant_III	182	302273	0.001	0.986	0.885	1.049	0.004	FALSE
Rekenvariant_II	161	302273	0.001	0.986	0.885	1.05	0.003	FALSE
Rekenvariant_I	151	302273	0	0.985	0.885	1.05	0.005	FALSE
International	670	302273	0.002	0.984	0.883	1.048	0.031	FALSE

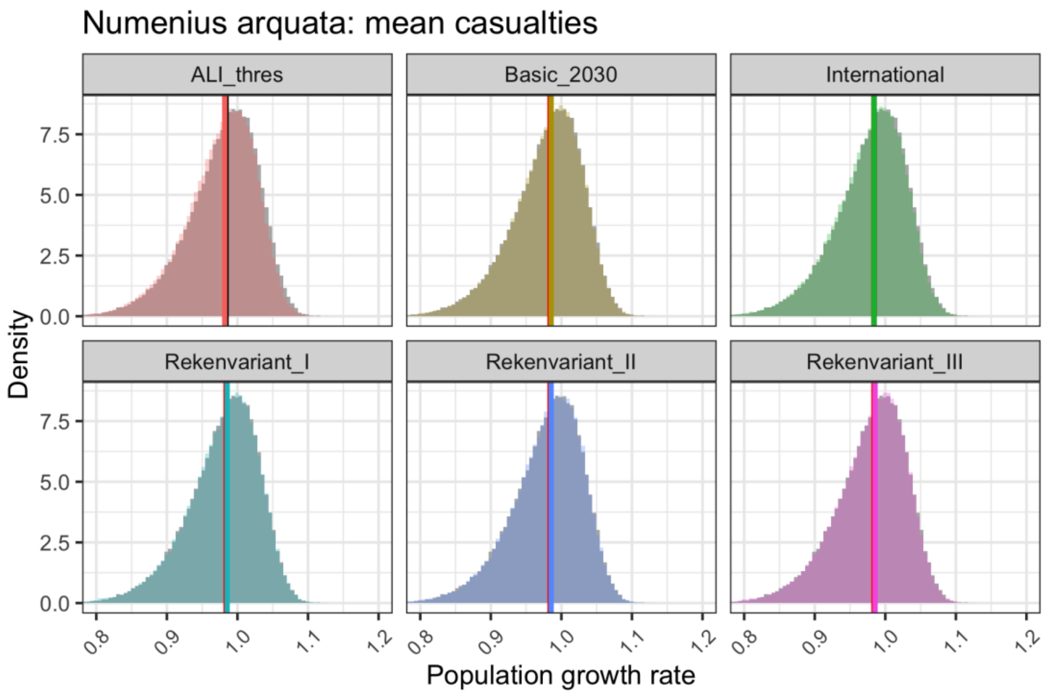

Figure 5.25 *Population growth rates per scenario for the Eurasian curlew (Numenius arquata). Within each panel the distribution of the unimpacted population growth rate (grey bars) is compared with the distribution of the impacted population growth rate (coloured bars). Vertical lines indicate median population growth rates for unimpacted (black) and impacted (coloured) populations and the ALI threshold population growth rate (red).*

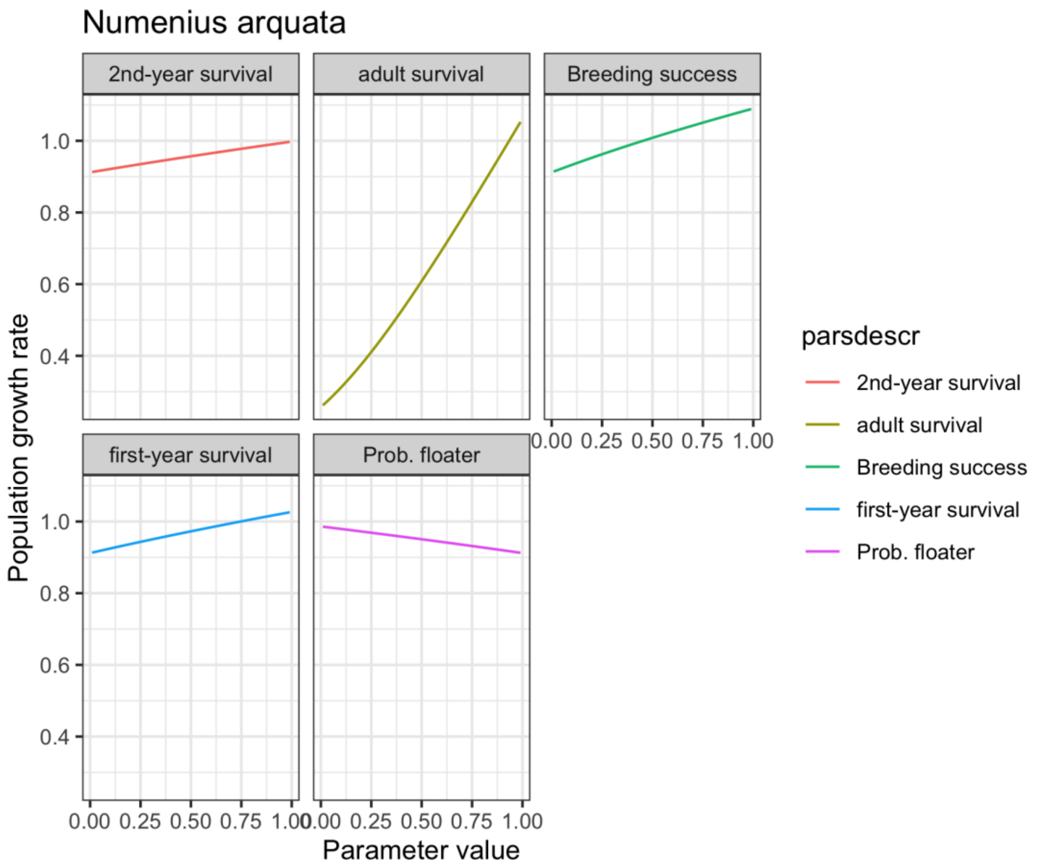

Figure 5.26 *Results of the sensitivity analysis for the Eurasian curlew* (Numenius arquata). *A steeper trend indicates a stronger effect on the population growth rate by a modification of the parameter.*

Black tern

Table 5.15 *Summary black tern population level effects; Casualties represent the mean number of casualties across time periods, Abundance represents the maximum number of birds across time periods used as population size, Mortality is the mortality probability due to collisions. The median, 5%and 95% percentiles of the population growth rates (lambda) are also reported. P causality represents the probability that a violation of the X threshold results from an OWF induced impact. The last column shows whether P causality violates the ALI threshold.*

Scenario	Casualties	Abundance	Mortality	Lambda median	5%	95%	P causality X = 30%	ALI 0.5
null	NA	NA	0	0.951	0.869	1.017	0	FALSE
Basic_2030	9	285482	0	0.951	0.869	1.017	0	FALSE
Rekenvariant_III	18	285482	0	0.951	0.869	1.016	0	FALSE
Rekenvariant_II	16	285482	0	0.951	0.869	1.017	0	FALSE
Rekenvariant_I	15	285482	0	0.951	0.869	1.016	0	FALSE
International	33	285482	0	0.951	0.869	1.016	0	FALSE

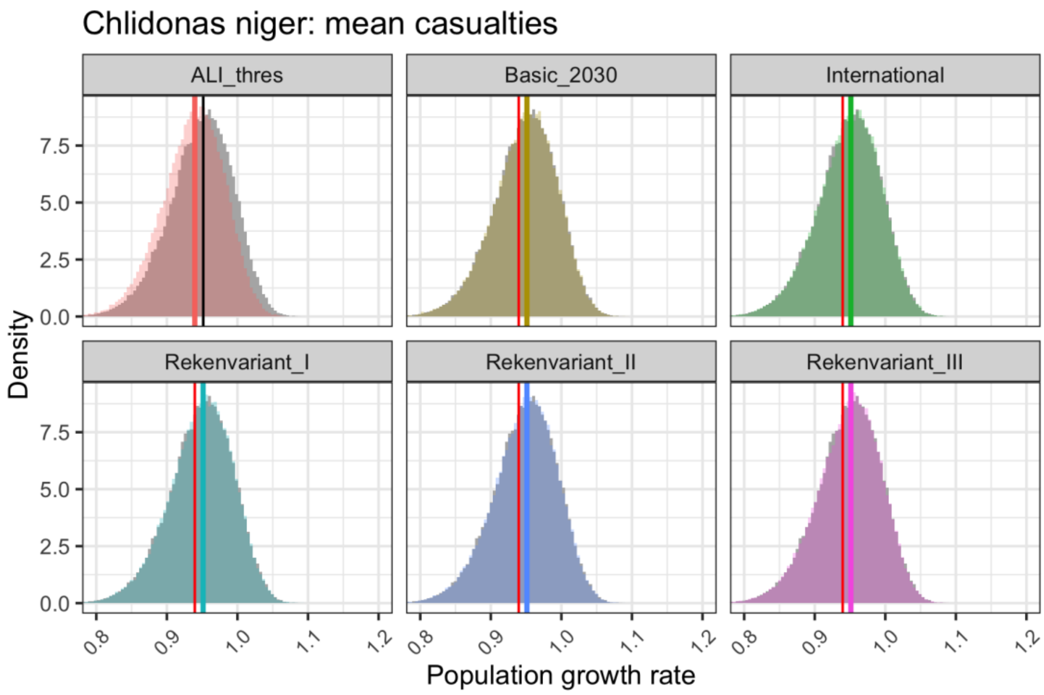

Figure 5.27 *Population growth rates per scenario for the black tern (Chlidonias niger). Within each panel the distribution of the unimpacted population growth rate (grey bars) is compared with the distribution of the impacted population growth rate (coloured bars). Vertical lines indicate median population growth rates for unimpacted (black) and impacted (coloured) populations and the ALI threshold population growth rate (red).*

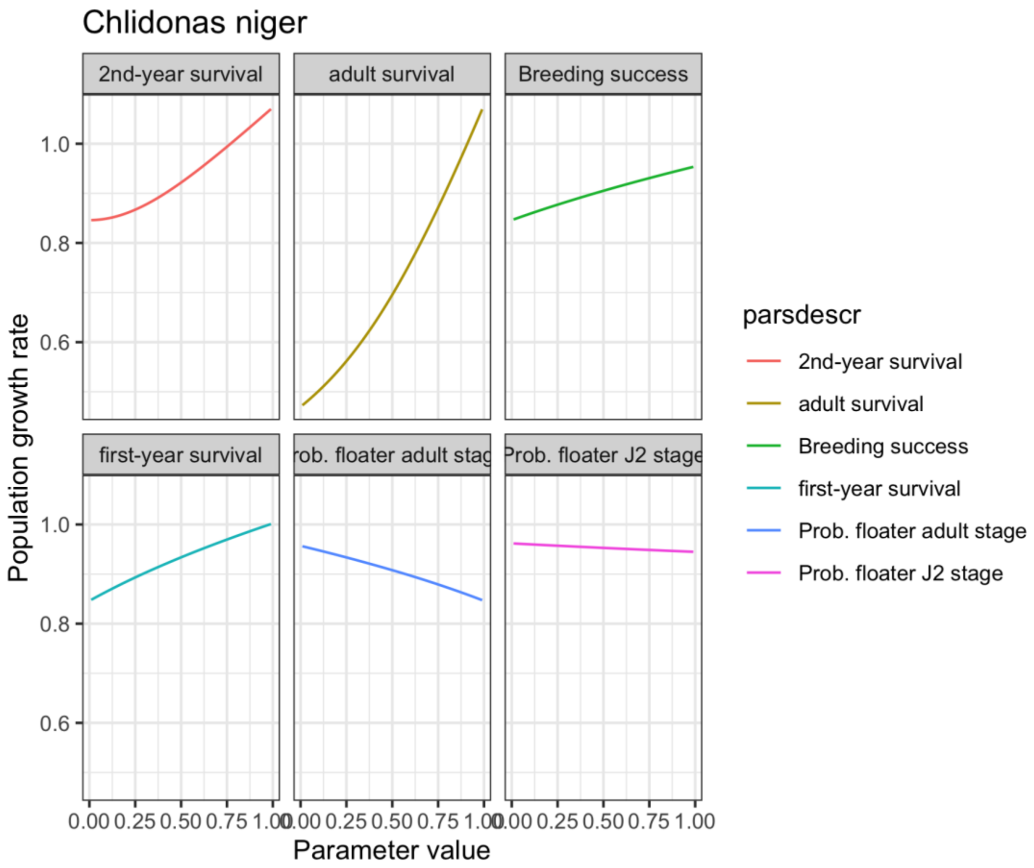

Figure 5.28 *Results of the sensitivity analysis the black tern (*Chlidonias niger*). A steeper trend indicates a stronger effect on the population growth rate by a modification of the parameter.*

Common starling

Table 5.16 *Summary common starling population level effects; Casualties represent the mean number of casualties across time periods, Abundance represents the maximum number of birds across time periods used as population size, Mortality is the mortality probability due to collisions. The median, 5% and 95% percentiles of the population growth rates (lambda) are also reported. P causality represents the probability that a violation of the X threshold results from an OWF induced impact. The last column shows whether P causality violates the ALI threshold.*

Scenario	Casualties	Abundance	Mortality	Lambda median	5%	95%	P causality X = 30%	ALI 0.5
null	NA	NA	0	0.836	0.544	1.097	0	FALSE
Basic_2030	3022	18501266	0	0.836	0.545	1.099	0	FALSE
Rekenvariant_III	6154	18501266	0	0.835	0.545	1.099	0.001	FALSE
Rekenvariant_II	5437	18501266	0	0.837	0.545	1.098	0	FALSE
Rekenvariant_I	5078	18501266	0	0.835	0.543	1.097	0.002	FALSE
International	22411	18501266	0.001	0.835	0.544	1.099	0.002	FALSE

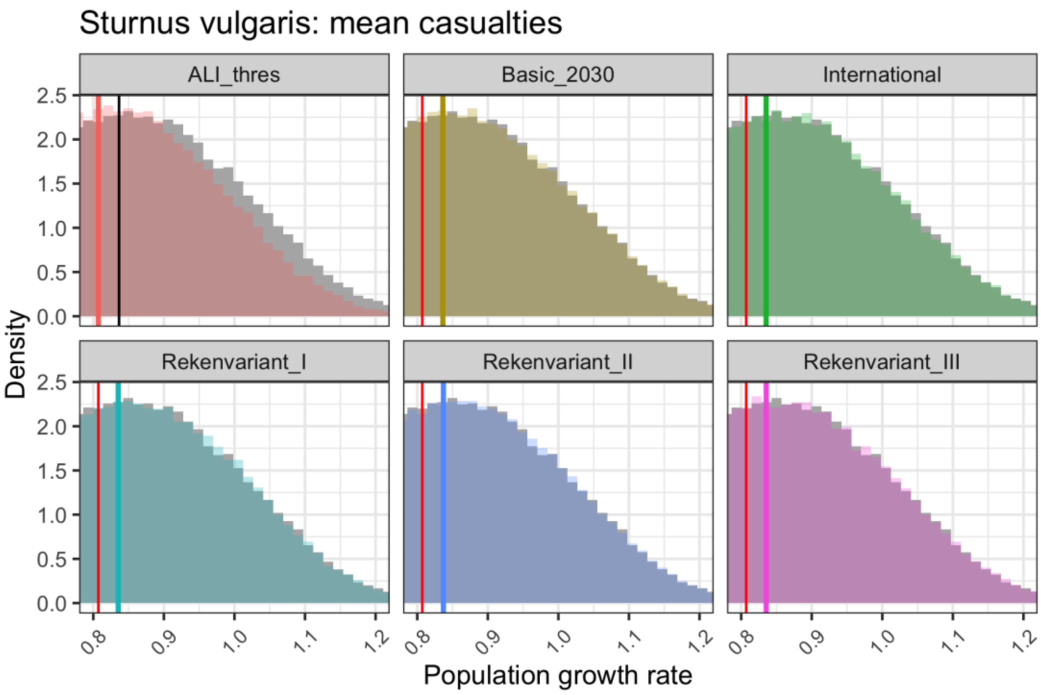

Figure 5.29 *Population growth rates per scenario for the common starling (Sturnus vulgaris). Within each panel the distribution of the unimpacted population growth rate (grey bars) is compared with the distribution of the impacted population growth rate (coloured bars). Vertical lines indicate median population growth rates for unimpacted (black) and impacted (coloured) populations and the ALI threshold population growth rate (red).*

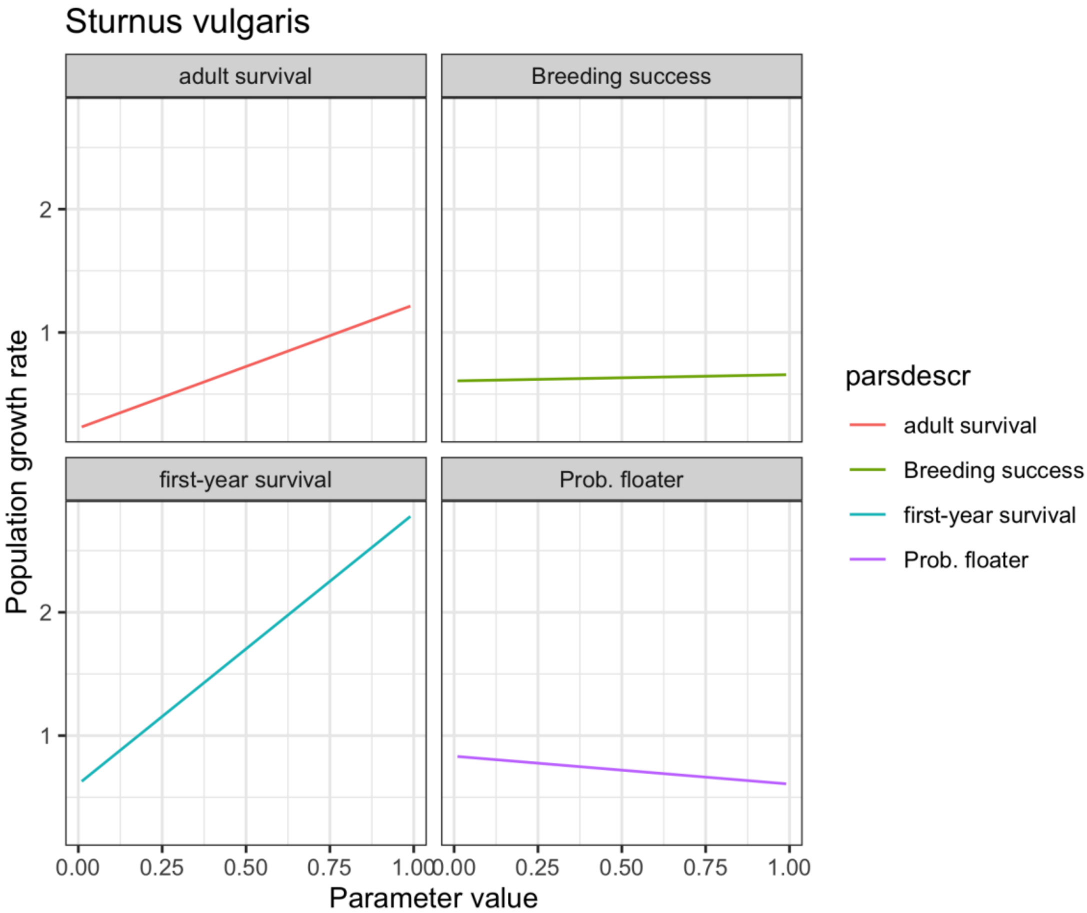

Figure 5.30 *Results of the sensitivity analysis for the common starling* (Sturnus vulgaris). *A steeper trend indicates a stronger effect on the population growth rate by a modification of the parameter.*

Bar-tailed godwit

Table 5.17 *Summary bar-tailed godwit population level effects; Casualties represent the mean number of casualties across time periods, Abundance represents the maximum number of birds across time periods used as population size, Mortality is the mortality probability due to collisions. The median, 5% and 95% percentiles of the population growth rates (lambda) are also reported. P causality represents the probability that a violation of the X threshold results from an impact. The last column shows whether P causality violates the ALI threshold.*

Scenario	Casualties	Abundance	Mortality	Lambda median	5%	95%	P causality X = 15%	ALI 0.1
null	NA	NA	0	0.998	0.958	1.036	0	FALSE
Basic_2030	99	347671	0	0.998	0.958	1.036	0.015	FALSE
Rekenvariant_III	199	347671	0.001	0.997	0.957	1.035	0.021	FALSE
Rekenvariant_II	176	347671	0.001	0.997	0.957	1.035	0.024	FALSE
Rekenvariant_I	165	347671	0	0.997	0.957	1.036	0.019	FALSE
International	729	347671	0.002	0.996	0.956	1.034	0.086	FALSE

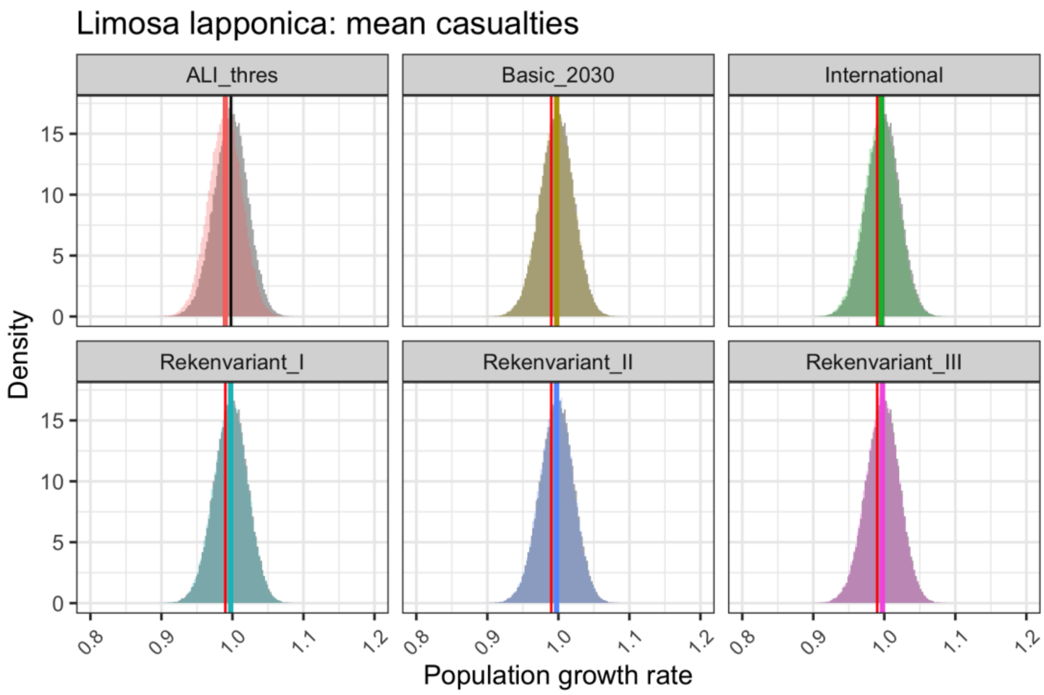

Figure 5.31 *Population growth rates per scenario for the bar-tailed godwit (Limosa lapponica). Within each panel the distribution of the unimpacted population growth rate (grey bars) is compared with the distribution of the impacted population growth rate (coloured bars). Vertical lines indicate median population growth rates for unimpacted (black) and impacted (coloured) populations and the ALI threshold population growth rate (red).*

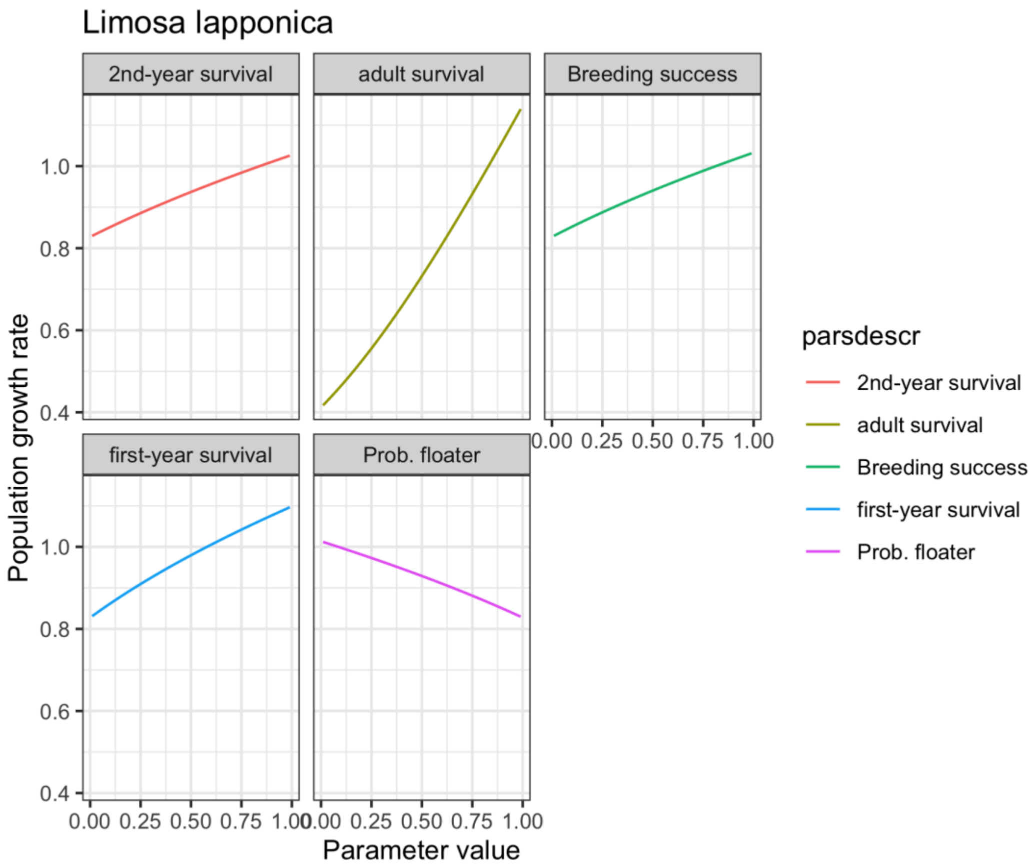

Figure 5.32 *Results of the sensitivity analysis for the bar-tailed godwit (*Limosa lapponica*). A steeper trend indicates a stronger effect on the population growth rate by a modification of the parameter.*

Red knot

Table 5.18 *Summary red knot population level effects; Casualties represent the mean number of casualties across time periods, Abundance represents the maximum number of birds across time periods used as population size, Mortality is the mortality probability due to collisions. The median, 5%and 95% percentiles of the population growth rates (lambda) are also reported. P causality represents the probability that a violation of the X threshold results from an OWF induced impact. The last column shows whether P causality violates the ALI threshold.*

Scenario	Casualties	Abundance	Mortality	Lambda median	5%	95%	P causality X = 30%	ALI 0.5
null	NA	NA	0	0.932	0.91	0.954	0	FALSE
Basic_2030	168	672197	0	0.932	0.91	0.954	0.02	FALSE
Rekenvariant_III	341	672197	0.001	0.932	0.91	0.954	0.054	FALSE
Rekenvariant_II	302	672197	0	0.932	0.91	0.954	0.037	FALSE
Rekenvariant_I	282	672197	0	0.932	0.91	0.954	0.029	FALSE
International	1245	672197	0.002	0.93	0.909	0.952	0.167	FALSE

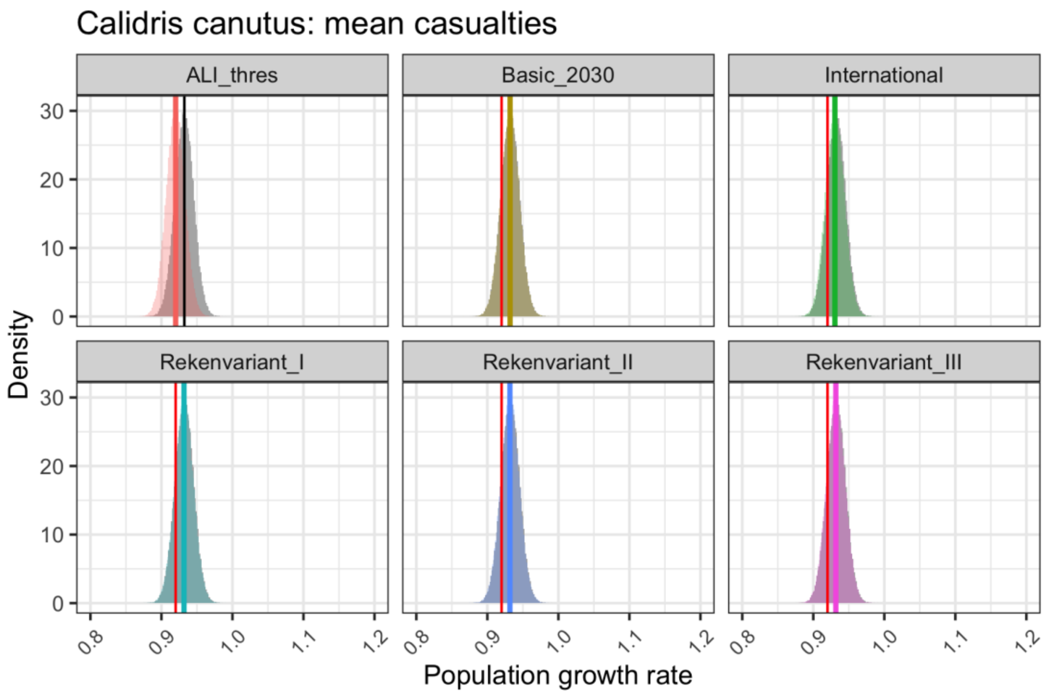

Figure 5.33 *Population growth rates per scenario for the red knot (Calidris canutus). Within each panel the distribution of the unimpacted population growth rate (grey bars) is compared with the distribution of the impacted population growth rate (coloured bars). Vertical lines indicate median population growth rates for unimpacted (black) and impacted (coloured) populations and the ALI threshold population growth rate (red).*

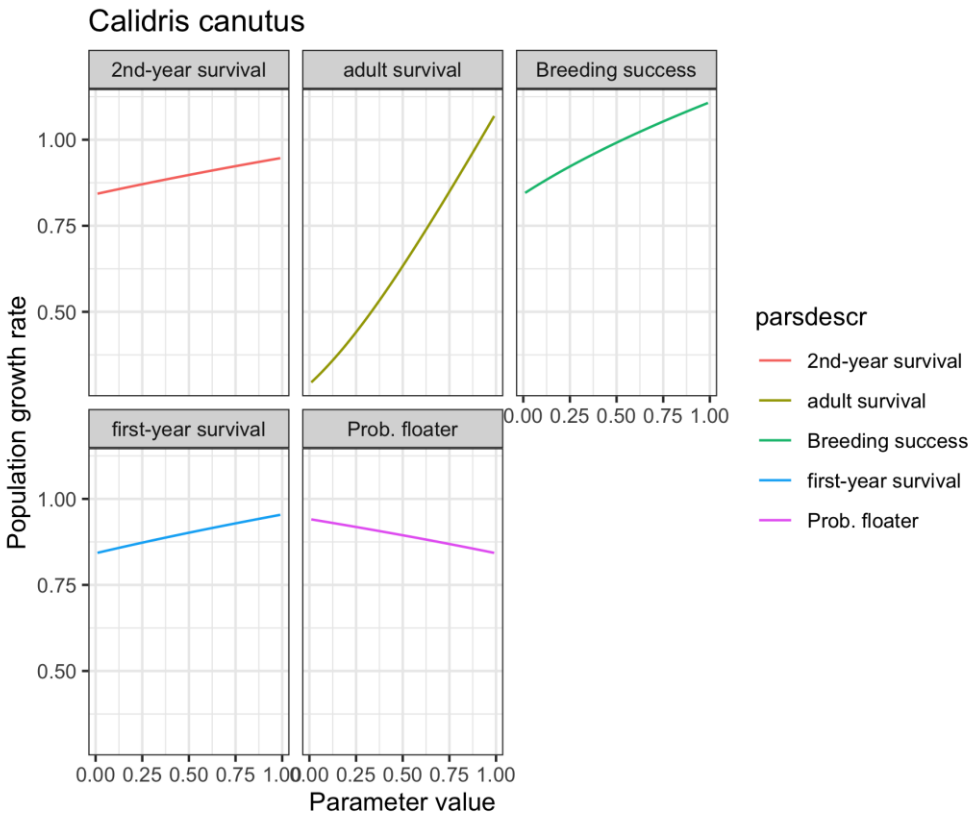

Figure 5.34 *Results of the sensitivity analysis for the red knot (Calidris canutus). A steeper trend indicates a stronger effect on the population growth rate by a modification of the parameter.*

5.2 Summary of assessments based on Acceptable Levels of Impact

In table 5.17 the summary of the species-specific assessments of §5.1 are summarised. For the herring gull and the northern gannet all scenarios result in a violation of the Acceptable Level of Impact (ALI). These results will be further analysed for the final report. For the great black-blacked gull this holds for all future national scenarios, but not for the basic scenario (comprising of existing and realistic wind farms until 2030, being part of the Roadmap 2030) and the international scenario. For the black-legged kittiwake, the two larger national scenarios violate the ALI, but the smallest national scenario and the international scenario do not. For all the other species, none of the scenarios violates the respective ALI's.

Table 5.17 Summary of assessments for the species-specific population level effects per scenario. TRUE = violation of the ALI threshold; FALSE = no violation of the ALI threshold.

Species	Scenario				
	Basic Nat 30	Rekenvariant III	Rekenvariant II	Rekenvariant I	Int 30
Great black-backed gull	FALSE	TRUE	FALSE	FALSE	FALSE
Lesser black-backed gull	FALSE	FALSE	FALSE	FALSE	FALSE
Herring gull	TRUE	TRUE	TRUE	TRUE	TRUE
Little gull	FALSE	FALSE	FALSE	FALSE	FALSE
Black-legged kittiwake	FALSE	TRUE	FALSE	FALSE	FALSE
Northern gannet	TRUE	TRUE	TRUE	TRUE	TRUE
Great skua	FALSE	FALSE	FALSE	FALSE	FALSE
Arctic skua	FALSE	FALSE	FALSE	FALSE	FALSE
Common tern	FALSE	FALSE	FALSE	FALSE	FALSE
Sandwich tern	FALSE	FALSE	FALSE	FALSE	FALSE
Bewick's swan	FALSE	FALSE	FALSE	FALSE	FALSE
Brent goose	FALSE	FALSE	FALSE	FALSE	FALSE
Common shelduck	FALSE	FALSE	FALSE	FALSE	FALSE
Curlew	FALSE	FALSE	FALSE	FALSE	FALSE
Red knot	FALSE	FALSE	FALSE	FALSE	FALSE
Black tern	FALSE	FALSE	FALSE	FALSE	FALSE
Common starling	FALSE	FALSE	FALSE	FALSE	FALSE

References

Alerstam, T., M. Rosén, J. Bäckman, P.G.P. Ericson & O. Hellgren, 2007. Flight Speeds among Bird Species: Allometric and Phylogenetic Effects. PLoS Biology 5(8): e197. doi: 10.1371/journal.pbio.0050197.

Band, W., M. Madders & D.P. Whitfield, 2007. Developing field and analystical methods to assess avian collision risk at wind farms. in I.M. de Lucas,G.F.E. Janss &M.F. (eds) (Ed.). *Birds and wind farms. Risk Assessment and Mitigation*. Blz. 275. Quercus. Madrid, Spain. pp 259-275.

Band, W., 2012. Using a collision risk model to assess bird collision risks for offshore windfarms. SOSS, The Crown Estate, London, Uk.

BirdLife International, 2004. Birds in Europe, population estimates, trends and conservation status. BirdLife Conservation Series No. 12. BirdLife International, Cambridge, UK.

BirdLife International, 2015. European Red List of Birds. BirdLife Conservation Series No. 12. Office for Official Publications of the European Communities, Luxembourg.

Blake, R.W. & K.H. Chan, 2006. Flight speeds of seven bird species during chick rearing. Canadian Journal of Zoology 84(7): 1047-1052.

Camphuysen, C.J. & M.F. Leopold, 1994. Atlas of seabirds in the southern North Sea. IBN resaerch report 94/6; NIOZ report 1994-8. IBN-DLO, NZG, NIOZ, Texel, Zeist.

Camphuysen, C.J., 2013. A historical ecology of two closely related gull species (Laridae): multiple adaptations to a man-made environment. Ph.D.-thesis. University of Groningen, Groningen.

Cleasby, I.R., E.D. Wakefield, S. Bearhop, T.W. Bodey, S.C. Votier & K.C. Hamer, 2015. Three-dimensional tracking of a wide-ranging marine predator: flight heights and vulnerability to offshore wind farms. Journal of Applied Ecology 52(6): 1474-1482.

Collins, P.M., L.G. Halsey, J.P.Y. Arnould, P.J.A. Shaw, S. Dodd & J.A. Green, 2016. Energetic consequences of time-activity budgets for a breeding seabird. Journal of Zoology DOI: 10.1111/jzo.12370.

Cook, A.S.C.P., E.M. Humphreys, F. Bennet, E.A. Masden & N.H.K. Burton, 2018. Quantifying avian avoidance of offshore wind turbines: Current evidence and key knowledge gaps. Marine Environmental Research 140: 278-288.

Duijns, S., L.J. Niles, A. Dey, Y. Aubry, C. Friis, S. Koch, A.M. Anderson & P.A. Smith, 2017. Body condition explains migratory performance of a long-distance migrant. Proceedings of the Royal Society B: Biological Sciences 284(1866): 20171374.

Fijn, R.C. & A. Gyimesi, 2018. Behaviour related flight speeds of Sandwich Terns and their implications for wind farm collision rate modelling and impact assessment. Environmental Impact Assessment Review 71: 12-16.

Furness, R.W., S. Garthe, M. Trinder, J. Matthiopoulos, S. Wanless & J. Jeglinski, 2018. Nocturnal flight activity of northern gannets *Morus bassanus* and implications for modelling collision risk at offshore wind farms. Environmental Impact Assessment Review 73: 1-6.

Garthe, S. & O. Hüppop, 2004. Scaling possible adverse effects of marine wind farms on seabirds: developing and applying a vulnerability index. Journal of Applied Ecology 41(4): 724-734.

Green, R.M.W., N.H.K. Burton & A.S.C.P. Cook, 2021. Migratory movements of British and Irish Common Shelduck *Tadorna tadorna*: a review of ringing data and a pilot tracking study to inform potential interactions with offshore wind farms in the North Sea. Ringing & Migration 34(2): 71-83.

Gyimesi, A., J.W. de Jong & R.C. Fijn, 2017a. Review and analysis of tracking data to delineate flight characteristics and migration routes of birds over the Southern North Sea. report nr. 16-139. Bureau Waardenburg, Culemborg.

Gyimesi, A., J.W. de Jong & R.C. Fijn, 2017b. Validation of biological variables for use in the SOSS Band model for Lesser Black-backed Gull *Larus fuscus* and Herring Gull *Larus argentatus*. report nr. 16-042. Bureau Waardenburg, Culemborg.

Horswill, C. & R.A. Robinson, 2015. Review of seabird demographic rates and density dependence. JNCC Report No. 552. Joint Nature Conservation Committee, Peterborough.

Johnston, A., A.S.C.P. Cook, L.J. Wright, E.M. Humphreys & N.H.K. Burtan, 2014. Modelling flight heights of marine birds to more accurately assess collision risk with offshore wind turbines. Journal of Applied Ecology 51: 31-41.

van Kooten, T., F. Soudijn, I. Tulp, C. Chen, D. Benden & M. Leopold, 2019. The consequences of seabird habitat loss from offshore wind turbines. Report C063/19. Wageningen Marine Research, IJmuiden.

Leopold, M.F., M.P. Collier, A. Gyimesi, R.H. Jongbloed, M.J.M. Poot, v.d.W. J.T. & M. Scholl, 2015. Iteration cycle: Dealing with peaks in counts of birds following active fishing vessels when assessing cumulative effects of offshore wind farms and other human activities in the Southern North Sea. Additional note to IMARES Report C166/14 IMARES, Wageningen.

Maclean, I.M.D., L.J. Wright, D.A. Showler & M.M. Rehfisch, 2009. A review of assessment methodologies for offshore windfarms. BTO Report commissioned by COWRIE Ltd. BTO

Marine Scotland, 2018. Stochastic Band CRM – GUI User manual. Available at https://www2.gov.scot/Topics/marine/marineenergy/mre/current/StochasticCRM

Maynard, L.D., 2018. Internal and external factors influencing foraging ecology of North Atlantic large Laridae. MSc Thesis. University of Manitoba.

Pennycuick, C.J., 1990. Predicting wingbeat frequency and wavelength of birds. Journal of Experimental Biology 150: 171-185.

Pennycuick, C.J., S. Åkesson & A. Hedenström, 2013. Air speeds of migrating birds observed by ornithodolite and compared with predictions from flight theory. Journal of the Royal Society Interface 10(86): 20130419.

Potiek, A., M.P. Collier, H. Schekkerman & R.C. Fijn, 2019a. Effects of turbine collision mortality on population dynamics of 13 bird species. Bureau Waardenburg Report 18-342, Bureau Waardenburg, Culemborg.

Potiek, A., N. Vanermen, R.P. Middelveld, J. de Jong, E.W.M. Stienen & R.C. Fijn, 2019b. Spatial and temporal distribution of different age classes of seabirds in the North Sea. Analysis of ESAS database, Rapport 19-129. Bureau Waardenburg, Culemborg.

Potiek, A., G.J. IJntema, T. van Kooten, M.F. Leopold & M.P. Collier, 2021. Acceptable Levels of Impact from offshore wind farms on the Dutch Continental Shelf for 21 bird species. A novel approach for defining acceptable levels of additional mortality from turbine collisions and avoidance-induced habitat loss, Rapport 21-0120. Bureau Waardenburg, Culemborg.

R Core Team, 2019. A language and environment for statistical computing. R Foundation for Statistical Computing, Vienna, Austria.

Rijkswaterstaat, 2015. Kader Ecologie en Cumulatie t.b.v. uitrol windenergie op zee Deelrapport B - Bijlage Imares onderzoek Cumulatieve effecten op vogels en vleermuizen. Ministerie van Economische Zaken en Ministerie van Infrastructuur en Milieu, Den Haag.

Rijkswaterstaat, 2019. Kader Ecologie en Cumulatie t.b.v. uitrol windenergie op zee, KEC 3.0. Rijkswaterstaat in opdracht van het Ministerie van Landbouw, Natuur en Voedselkwaliteit, Den Haag.

Ross-Smith, V.H., C.B. Thaxter, E.A. Masden, J. Shamoun-Baranes, N.H.K. Burton, L.J. Wright, M.M. Rehfisch & A. Johnston, 2016. Modelling flight heights of Lesser Black-backed Gulls and Great Skuas from GPS: a Bayesian approach. Journal of Applied Ecology 53(6): 1676-1685.

Schwemmer, P., L. Enners & S. Garthe, 2016. Migration routes of Eurasian Curlews (*Numenius arquata*) resting in the eastern Wadden Sea based on GPS telemetry. Journal of Ornithology. 1-5.

Searle, K.R., A. Butler, D.C. Mobbs, M. Trinder, J. Waggitt, P. Evans & F. Daunt, 2019. Scottish Waters East Region Regional Sectoral Marine Plan Strategic Ornithology Study: final report. Centre for Ecology & Hydrology, Midlothian.

Skov, H., S. Heinanen, T. Norman, R.M. Ward, S. Mendez-Roldan & I. Ellis, 2018. ORJIP Bird Collision and Avoidance Study. Final report–April 2018. The Carbon Trust, United Kingdom.

Snow, D.W. & C.M. Perrins (eds), 1998. The Birds of the Western Palearctic. Concise Edition. Volume 1 Non-Passerines. Great Crested Grebe *Podiceps cristatus*. Oxford University Press, New York.

Wakeling, J.M. & J. Hodgson, 1992. Optimisation of the flight speed of the little, common and Sandwich tern. Journal of Experimental Biology 169: 261-266.

van der Wal, J.T., R.C. Fijn, A. Gyimesi & M. Scholl, 2015. 2nd Iteration: Effect of turbine capacity on collision numbers for three large gull species, based on revised density data, when assessing cumulative effects of offshore wind farms on birds in the southern North Sea. Additional note to IMARES Report C166/14 IMARES, Wageningen.

Appendix I

Wind Farm	Capacity MW (Max)	Num Turbines (Max)
Borssele 1	376	47
Borssele 2	376	47
Borssele 3	366.0	39
Borssele 4 - Blauwwind	366.0	39
Borssele Site V -Two towers	19	2
Egmond aan Zee	108	36
Eneco Luchterduinen	129	43
Gemini Zee energie	300	75
Gemini Buitengaats	300	75
Hollandse Kust Noord (Tender 2019)	700	69
Hollandse Kust West - (Tender 2020/2021)	1400	117
Hollandse Kust Zuid Holland I	385	70
Hollandse Kust Zuid Holland II	385	70
Hollandse Kust Zuid Holland III	385	70
Hollandse Kust Zuid Holland IV	385	70
IJmuiden Ver	4000	267
Prinses Amaliawindpark	120	60
Ten noorden van de Waddeneilanden - (Tender 2022)	700	47
Hollandse Kust West zuidelijke punt	700	47
Zoekgebied 1 Noord	4000	200
Zoekgebied 1 Zuid	2000	100
Zoekgebied 2 Noord	4000	200
Zoekgebied 5 Oost origineel	4000	267
IJmuiden Ver Noord	2000	134
Thornton Bank phase I	30	6
Northwind	216	72
Belwind	165	55
Norther	370	44
Rentel	309.0	42
Seamade (SeaStar)	252	30
Seamade (Mermaid)	235	28
Nobelwind	165	50
Thornton Bank phase II	185	30
Thornton Bank phase III	110.7	18
Northwester 2	219.0	23
Princess Elisabeth - Noordhinder Noord - 2023 Tender	700	59
Princess Elisabeth - Fairybank/Nordhinder Zuid - 2025 Tender	1400	94
Albatros	112	16
Alpha Ventus	60	12
Amrumbank West	302	80
BARD Offshore 1	400	80

Wind Farm	Capacity MW (Max)	Num Turbines (Max)
Borkum Riffgrund 1	312	78
Borkum Riffgrund 2	450	56
Borkum Riffgrund 3	900	81
Butendiek	288	80
DanTysk	288	80
Deutsche Bucht	252	31
EnBW He Dreiht	900	70
Global Tech I	400	80
Gode Wind 1 and 2	582	97
Gode Wind 3	241.75	22
Hohe See	497	71
Kaskasi	342	38
Meerwind Süd/Ost	288	80
Merkur	396	66
N-10.1	1000	57
N-10.2	700	47
N-13-3	1000	50
N-3.5	420	28
N-3.6	480	32
N-3.7	225	15
N-3.8	433	29
N-6.6	630	42
N-6.7	270	18
N-7.2	930	62
N-8.4	425	28
N-9.1	1000	67
N-9.2	1000	67
N-9.3	1000	67
N-9.4	1000	67
Nordergründe	110.7	18
Nordsee One	332.1	54
Nordsee Ost	295.2	48
Riffgat	108	30
Sandbank	288	72
Trianel Windpark Borkum I	200	40
Trianel Windpark Borkum II	203	32
Veja Mate	402	67
Horns Rev 1	160	80
Horns Rev 2	209.3	91
Horns Rev 3	406.7	49
Thor - 2020 Tender	1000	75
Vesterhav Nord/Syd	344	41
Dudgeon	402	67
Greater Gabbard	504	140

Wind Farm	Capacity MW (Max)	Num Turbines (Max)
Gunfleet Sands	173	48
Dogger Bank B	1200	95
Humber Gateway	219.0	73
Inner Dowsing	97.2	27
Kentish Flats	90	30
Lincs	270	75
London Array	630	175
Lynn	97	27
Race Bank	573	91
Dogger Bank C	1200	95
Sofia	1400	100
Hornsea Project Three	2400	231
Hornsea Project Two	1386	165
Scroby Sands	60	30
Sheringham Shoal	317	88
Teesside	62	27
Thanet	300	100
East Anglia Hub - ONE North	800	58
Triton Knoll	857	90
Westermost Rough	210	35
East Anglia Hub - TWO	900	65
Scottish Sectoral Marine Plan - E3	1000	50
Moray East	950	100
Seagreen	1140	114
Aberdeen Offshore Wind Farm (EOWDC)	93.2	11
Race Bank Extension	573	38
Dudgeon Extension	402	115
Sheringham Shoal Extension	317	16
Five Estuaries	353	18
North Falls	504	34
Kincardine - Phase 2	48	5
Seagreen 1A	360	36
Beatrice	588	84
Inch Cape	1000	72
Neart na Gaoithe	448	54
Kentish Flats Extension	49.5	15
Galloper	353	56
East Anglia ONE	714	102
East Anglia Hub - THREE	1400	100
Norfolk Vanguard	1800	158
Norfolk Boreas	1800	158
Blyth Offshore Demonstrator Phase 1	41.5	5
Berwick Bank	2300	115
Hywind Scotland Pilot Park	30	5

Wind Farm	**Capacity MW (Max)**	**Num Turbines (Max)**
Moray West	950	85
Blyth Offshore Demonstrator Phase 2	58.4	5
Dogger Bank A	1200	95
Hornsea Project One	1218	174